Supplementary Information

The secreted metabolome of *Streptomyces chartreusis* and implications for bacterial chemistry

Christoph H. R. Senges[1], Arwa Al-Dilaimi[2], Douglas H. Marchbank[3], Daniel Wibberg[2], Anika Winkler[2], Brad Haltli[3], Minou Nowrousian[4], Jörn Kalinowski[2], Russell G. Kerr[3], Julia E. Bandow[1]*

[1] Applied Microbiology, Ruhr University Bochum, 44780 Bochum, Germany
[2] Center for Biotechnology, Bielefeld University, 33594 Bielefeld, Germany
[3] Department of Chemistry, University of Prince Edward Island, Charlottetown, PE, C1A 4P3, Canada
[4] Department of General and Molecular Botany, Ruhr University Bochum, 44780 Bochum, Germany

Content

Supplementary tables

Tab. S1 Genome summary. Summary of information on the genome of *S. chartreusis* NRRL 3882.

length	8,983,317 bp
GC content	71.23%
annotated genes	7,940
tRNAs	79
rRNAs	18
in predicted biosynthesis clusters	3,060,457 bp 34.07%

Table S2: Biosynthesis cluster information. Summary of the antiSMASH biosynthesis cluster prediction for the genome of *S. chartreusis* NRRL 3882. Clusters for which products were found are marked in red. (page 1 of 6)

Cluster	Type	From	To	Most similar known cluster	MIBiG BGC-ID
1	Cf_putative	23240	40560	A54145_biosynthetic_gene_cluster (3% of genes show similarity)	BGC0000291_c1
2	Cf_putative	173240	186023	A54145_biosynthetic_gene_cluster (3% of genes show similarity)	BGC0000291_c1
3	Cf_putative	192600	210884	-	-
4	Lassopeptide	213513	236317	Alnumycin_biosynthetic_gene_cluster (6% of genes show similarity)	BGC0000195_c1
5	Cf_saccharide	332803	358039	-	-
6	Cf_putative	405285	422485	-	-
7	Cf_putative	422567	445607	-	-
8	Melanin	496290	506901	Melanin_biosynthetic_gene_cluster (42% of genes show similarity)	BGC0000908_c1
9	Cf_putative	576501	594899	-	-
10	Cf_putative	599891	606325	-	-
11	Cf_putative	726024	747072	-	-
12	T1pks	834590	882893	Lobophorin_biosynthetic_gene_cluster (6% of genes show similarity)	BGC0001183_c1
13	Cf_saccharide	929133	977696	Tallysomycin_biosynthetic_gene_cluster (5% of genes show similarity)	BGC0001048_c1
14	Cf_saccharide	999313	1036687	Tetronasin_biosynthetic_gene_cluster (3% of genes show similarity)	BGC0000163_c1
15	T3pks-Nrps	1021374	1094818	Coelichelin_biosynthetic_gene_cluster (100% of genes show similarity)	BGC0000325_c1
16	Cf_putative	1122096	1129289	-	-
17	Cf_saccharide	1132834	1168661	Meilingmycin_biosynthetic_gene_cluster (2% of genes show similarity)	BGC0000093_c1
18	Terpene-Cf_saccharide	1205879	1236826	Hopene_biosynthetic_gene_cluster (92% of genes show similarity)	BGC0000663_c1
19	Cf_putative	1254051	1260700	-	-
20	Cf_putative	1287320	1305082	GE81112_biosynthetic_gene_cluster (14% of genes show similarity)	BGC0000360_c1
21	Cf_saccharide	1374082	1400540	Sch47554_/_Sch47555_biosynthetic_gene_cluster (10% of genes show similarity)	BGC0000268_c1
22	T2pks	1407588	1450343	Granaticin_biosynthetic_gene_cluster (27% of genes show similarity)	BGC0000227_c1
23	Cf_saccharide-Amglyccycl	1421015	1475661	Granaticin_biosynthetic_gene_cluster (27% of genes show similarity)	BGC0000227_c1
24	Cf_fatty_acid	1492827	1513807	-	-
25	Cf_putative	1550732	1567450	-	-

Table S2: Biosynthesis cluster information. Summary of the antiSMASH biosynthesis cluster prediction for the genome of *S. chartreusis* NRRL 3882. Clusters for which products were found are marked in red. (page 2 of 6)

Cluster	Type	From	To	Most similar known cluster	MIBiG BGC-ID
26	Cf_putative	1605165	1619242	Kanamycin_biosynthetic_gene_cluster (15% of genes show similarity)	BGC0000704_c1
27	Cf_putative	1700448	1714088	Lipomycin_biosynthetic_gene_cluster (9% of genes show similarity)	BGC0001003_c1
28	Siderophore	1736990	1752570	-	-
29	Other	1756539	1797297	Meilingmycin_biosynthetic_gene_cluster (3% of genes show similarity)	BGC0000093_c1
30	Cf_saccharide	1817459	1847309	-	-
31	Terpene	1990654	2012816	-	-
32	Bacteriocin	2073611	2097275	Enduracidin_biosynthetic_gene_cluster (4% of genes show similarity)	BGC0000341_c1
33	Cf_saccharide	2102364	2124664	Enduracidin_biosynthetic_gene_cluster (14% of genes show similarity)	BGC0000341_c1
34	Cf_putative	2170905	2210925	JBIR-34,_JBIR-35_biosynthetic_gene_cluster (12% of genes show similarity)	BGC0000376_c1
35	Cf_saccharide	2232701	2285215	-	-
36	Siderophore	2359453	2371666	-	-
37	Cf_saccharide	2626814	2648124	Frankiamicin_biosynthetic_gene_cluster (21% of genes show similarity)	BGC0001197_c1
38	Cf_putative	2681544	2693681	-	-
39	T1pks-Cf_fatty_acid - Butyrolactone	2727323	2782452	Stambomycin_biosynthetic_gene_cluster (16% of genes show similarity)	BGC0000151_c1
40	T2pks	2814298	2856813	Spore_pigment_biosynthetic_gene_cluster (75% of genes show similarity)	BGC0000271_c1
41	Cf_putative	2994518	3003271	Echosides_biosynthetic_gene_cluster (35% of genes show similarity)	BGC0000340_c1
42	Terpene	3038256	3059341	Albaflavenone_biosynthetic_gene_cluster (100% of genes show similarity)	BGC0000660_c1
43	Cf_saccharide	3102118	3123869	-	-
44	Cf_putative	3154745	3174277	-	-
45	Nucleoside-Cf_saccharide	3257787	3282146	Tunicamycin_biosynthetic_gene_cluster (85% of genes show similarity)	BGC0000880_c1
46	Cf_saccharide	3316387	3340512	Cypemycin_biosynthetic_gene_cluster (22% of genes show similarity)	BGC0000582_c1
47	Cf_putative	3349881	3356835	-	-
48	Cf_saccharide	3403022	3425505	-	-
49	Cf_putative	3455602	3474041	-	-
50	Cf_putative	3536975	3565666	-	-

Table S2: Biosynthesis cluster information. Summary of the antiSMASH biosynthesis cluster prediction for the genome of *S. chartreusis* NRRL 3882. Clusters for which products were found are marked in red. (page 3 of 6)

Cluster	Type	From	To	Most similar known cluster	MIBiG BGC-ID
51	Cf_saccharide	3707184	3728491	-	-
52	Cf_saccharide	3751708	3773918	-	-
53	Cf_saccharide	3781103	3803034	-	-
54	Nrps	3808020	3850002	-	-
55	Cf_putative	3889468	3910342	-	-
56	Cf_saccharide	4009221	4030114	Gilvocarcin_biosynthetic_gene_cluster (7% of genes show similarity)	BGC0000226_c1
57	Cf_saccharide	4229097	4249753	-	-
58	Cf_saccharide	4298337	4323559	Zorbamycin_biosynthetic_gene_cluster (8% of genes show similarity)	BGC0001058_c1
59	Cf_saccharide	4349243	4388463	A54145_biosynthetic_gene_cluster (5% of genes show similarity)	BGC0000291_c1
60	Butyrolactone	4497002	4508054	Griseoviridin_/_viridogrisein_biosynthetic_gene_cluster (8% of genes show similarity)	BGC0000459_c1
61	Cf_putative	4631705	4647088	-	-
62	Cf_saccharide	4662330	4683289	-	-
63	Cf_saccharide	4692936	4714660	Clavulanic_acid_biosynthetic_gene_cluster (8% of genes show similarity)	BGC0000845_c1
64	Cf_saccharide	4899873	4921294	-	-
65	Cf_putative	4933100	4940465	-	-
66	Cf_saccharide	4946700	4967644	-	-
67	Cf_putative	4999656	5029511	Kosinostatin_biosynthetic_gene_cluster (4% of genes show similarity)	BGC0001073_c1
68	Cf_putative	5056938	5075965	-	-
69	Cf_putative	5091906	5112623	-	-
70	Cf_saccharide	5115568	5137028	Cinnamycin_biosynthetic_gene_cluster (14% of genes show similarity)	BGC0000503_c1
71	Thiopeptide-Lantipeptide	5148607	5198127	Platencin_biosynthetic_gene_cluster (9% of genes show similarity)	BGC0001156_c1
72	Cf_putative	5252521	5267752	-	-
73	Cf_putative	5295608	5302772	-	-
74	Cf_putative	5350993	5371873	Siomycin_biosynthetic_gene_cluster (7% of genes show similarity)	BGC0000655_c1
75	Cf_saccharide	5409224	5430267	-	-

Table S2: Biosynthesis cluster information. Summary of the antiSMASH biosynthesis cluster prediction for the genome of *S. chartreusis* NRRL 3882. Clusters for which products were found are marked in red. (page 4 of 6)

Cluster	Type	From	To	Most similar known cluster	MIBiG BGC-ID
76	Cf_saccharide	5482688	5524918	-	-
77	Cf_saccharide	5531260	5553635	-	-
78	Cf_saccharide	5651601	5673607	-	-
79	Siderophore	5728969	5743480	Desferrioxamine_B_biosynthetic_gene_cluster (100% of genes show similarity)	BGC0000940_c1
80	Cf_saccharide-Melanin	5817869	5853889	Melanin_biosynthetic_gene_cluster (60% of genes show similarity)	BGC0000909_c1
81	Cf_saccharide	6002584	6023792	-	-
82	Lassopeptide	6075771	6098560	-	-
83	Cf_putative	6145635	6164789	-	-
84	Terpene-Nrps-Cf_saccharide	6178346	6239867	SCO-2138_biosynthetic_gene_cluster (92% of genes show similarity)	BGC0000595_c1
85	Cf_fatty_acid	6262817	6284345	Fredericamycin_biosynthetic_gene_cluster (6% of genes show similarity)	BGC0000224_c1
86	Cf_saccharide	6316501	6366056	-	-
87	Cf_putative	6366239	6375787	Platencin_biosynthetic_gene_cluster (6% of genes show similarity)	BGC0001156_c1
88	Nrps-T1pks	6393467	6444104	Rifamycin_biosynthetic_gene_cluster (12% of genes show similarity)	BGC0000136_c1
89	Cf_saccharide	6538442	6560097	-	-
90	Cf_saccharide	6592205	6613524	-	-
91	Cf_putative	6625323	6642789	-	-
92	Cf_saccharide	6649649	6670746	-	-
93	Cf_putative	6737016	6745860	-	-
94	Cf_putative	6806690	6812867	Paromomycin_biosynthetic_gene_cluster (5% of genes show similarity)	BGC0000712_c1
95	Terpene	6826993	6848153	-	-
96	Cf_putative	6919044	6926625	-	-
97	Ectoine	6960000	6970398	Ectoine_biosynthetic_gene_cluster (75% of genes show similarity)	BGC0000853_c1
98	Cf_putative	6992575	7009930	-	-
99	Cf_saccharide	7059287	7080432	Scabichelin_biosynthetic_gene_cluster (30% of genes show similarity)	BGC0000423_c1
100	Cf_putative	7090595	7095058	UK-68,597_biosynthetic_gene_cluster (4% of genes show similarity)	BGC0001178_c1

Table S2: Biosynthesis cluster information. Summary of the antiSMASH biosynthesis cluster prediction for the genome of *S. chartreusis* NRRL 3882. Clusters for which products were found are marked in red. (page 5 of 6)

Cluster	Type	From	To	Most similar known cluster	MIBiG BGC-ID
101	Cf_saccharide	7121037	7147090	-	-
102	Cf_putative	7159737	7168952	-	-
103	Cf_putative	7178654	7185364	-	-
104	Cf_putative	7192906	7197539	-	-
105	Cf_putative	7327666	7347855	Streptomycin_biosynthetic_gene_cluster (9% of genes show similarity)	BGC0000717_c1
106	Cf_saccharide	7367583	7389850	-	-
107	Cf_putative	7447059	7456919	-	-
108	Cf_saccharide	7464954	7500646	-	-
109	Cf_putative	7582886	7590962	Kirromycin_biosynthetic_gene_cluster (3% of genes show similarity)	BGC0001070_c1
110	Cf_putative	7621529	7645776	-	-
111	Cf_putative	7720756	7726239	Herboxidiene_biosynthetic_gene_cluster (3% of genes show similarity)	BGC0001065_c1
112	T1pks	7796901	7892757	Calcimycin_biosynthetic_gene_cluster (100% of genes show similarity)	BGC0000032_c1
113	Cf_putative	7930155	7953004	-	-
114	Cf_putative	8102874	8114289	-	-
115	Cf_putative	8117762	8128535	-	-
116	Cf_putative	8174644	8185905	-	-
117	Cf_saccharide	8211895	8234579	-	-
118	Cf_putative	8235448	8300245	Yatakemycin_biosynthetic_gene_cluster (6% of genes show similarity)	BGC0000466_c1
119	Cf_putative	8316757	8327018	-	-
120	Terpene	8400535	8421605	Versipelostatin_biosynthetic_gene_cluster (5% of genes show similarity)	BGC0001204_c1
121	Bacteriocin-Lantipeptide-Cf_saccharide	8450351	8500179	Informatipeptin_biosynthetic_gene_cluster (100% of genes show similarity)	BGC0000518_c1
122	Cf_putative	8505757	8520562	-	-
123	T1pks	8552652	8596677	Maduropeptin_biosynthetic_gene_cluster (3% of genes show similarity)	BGC0001008_c1
124	Cf_saccharide	8628530	8650002	A-500359s_biosynthetic_gene_cluster (5% of genes show similarity)	BGC0000949_c1
125	T3pks	8649961	8691346	-	-

Table S2: Biosynthesis cluster information. Summary of the antiSMASH biosynthesis cluster prediction for the genome of *S. chartreusis* NRRL 3882. Clusters for which products were found are marked in red. (page 6 of 6)

Cluster	Type	From	To	Most similar known cluster	MIBiG BGC-ID
126	Cf_putative	8733683	8741218	-	-
127	Cf_putative	8875738	8889232	-	-
128	Cf_putative	8896783	8916705	-	-

Table S3: Summary of mass spectrometric identification. Data gathered on all identified compounds. Nomenclature in italics indicate compounds discovered in this study. The newly isolated compound is indicated by bold letters.

Name	Measured mass $[M+H]^+$	Theoretical mass $[M+H]^+$	Δppm	Sum formula $[+H]^+$	Reference & PubChem identifier
Calcimycin					
Calcimycin	524.2763	524.2761	0.381	$C_{29}H_{38}N_3O_6$	1,2
***Cal-01* (deoxacalcimycin)**	513.2596	513.2601	0.974	$C_{28}H_{37}N_2O_7$	*this study*
N-demethyl-calcimycin	510.2597	510.2604	1.372	$C_{28}H_{36}N_3O_6$	1,2
Cezomycin	495.2496	495.2495	0.202	$C_{28}H_{35}N_2O_6$	1,2
Cal-02	494.2645	494.2655	2.023	$C_{28}H_{36}N_3O_5$	*this study*
Tunicamycin					
Tuni-01 18:1	873.4699	873.4709	1.145	$C_{41}H_{69}N_4O_{16}$	*this study*
Tunicamycin D	859.4554	859.4552	0.233	$C_{40}H_{67}N_4O_{16}$	CID 56927841
Tuni-02 16:0	847.4555	847.4552	0.354	$C_{39}H_{67}N_4O_{16}$	*this study*
Tunicamycin B	845.4402	845.4396	0.710	$C_{39}H_{65}N_4O_{16}$	CID 56927836
Tunicamycin VI	833.4388	833.4396	0.960	$C_{38}H_{65}N_4O_{16}$	CID 56927835
Tunicamycin A	831.4263	831.4239	2.887	$C_{38}H_{63}N_4O_{16}$	CID 11104835
Tuni-03 14:0	819.4261	819.4239	2.685	$C_{37}H_{63}N_4O_{16}$	*this study*
Tuni-04 13:0	805.4073	805.4083	1.242	$C_{36}H_{61}N_4O_{16}$	*this study*
Tunicamycin I	803.3934	803.3926	0.996	$C_{36}H_{59}N_4O_{16}$	CID 56927848
Desferrioxamine					
Desf-01	633.3817	633.3823	0.947	$C_{28}H_{53}N_6O_{10}$	*this study*
Desferrioxamine G1	619.3661	619.3667	0.969	$C_{27}H_{51}N_6O_{10}$	3
Desferrioxamine D1	603.3706	603.3718	1.989	$C_{27}H_{51}N_6O_9$	CID 10008761
Desferrioxamine E	601.3572	601.3561	1.829	$C_{27}H_{49}N_6O_9$	3
Desf-02	599.3407	599.3405	0.334	$C_{27}H_{47}N_6O_9$	*this study*
Desferrioxamine D2	587.3411	587.3405	1.022	$C_{26}H_{47}N_6O_9$	4
Desf-03	585.3613	585.3612	0.171	$C_{27}H_{49}N_6O_8$	*this study*
Desf-04	577.3570	577.3561	1.559	$C_{25}H_{49}N_6O_9$	*this study*
Desf-05	575.3762	575.3768	1.043	$C_{26}H_{51}N_6O_8$	*this study*
Desferrioxamine X1/7	573.3251	573.3248	0.523	$C_{25}H_{45}N_6O_9$	4
Desferrioxamine B	561.3621	561.3612	1.603	$C_{25}H_{49}N_6O_8$	3
Desferrioxamine A1	547.3455	547.3455	0.000	$C_{24}H_{47}N_6O_8$	4
Desferrioxamine uA1	545.3658	545.3663	0.917	$C_{25}H_{49}N_6O_7$	4
Desf-06	537.3605	537.3612	1.303	$C_{23}H_{49}N_6O_8$	*this study*
Desferrioxamine A2	533.3291	533.3299	1.500	$C_{23}H_{45}N_6O_8$	4
Desf-07	518.3184	518.3190	1.158	$C_{23}H_{44}N_5O_8$	*this study*
Desf-08	493.3344	493.3350	1.216	$C_{21}H_{45}N_6O_7$	*this study*
Bisucaberin					
Ferrioxamine H	461.2611	461.2611	0.000	$C_{20}H_{37}N_4O_8$	5
Bisu-01	443.2491	443.2506	3.384	$C_{20}H_{35}N_4O_7$	*this study*
Bisu-02	433.2662	433.2662	0.000	$C_{19}H_{37}N_4O_7$	*this study*
Bisu-03	429.2344	429.2349	1.165	$C_{19}H_{33}N_4O_7$	*this study*
Bisucaberin	401.2392	401.2400	1.994	$C_{18}H_{33}N_4O_6$	6
Bisu-04	389.2389	389.2400	2.826	$C_{17}H_{33}N_4O_6$	*this study*
dDFx[00-]	361.2441	361.2451	2.768	$C_{16}H_{33}N_4O_5$	7
Bisu-05	345.2495	345.2502	2.028	$C_{16}H_{33}N_4O_4$	*this study*
Bisu-06	303.2403	303.2396	2.308	$C_{14}H_{31}N_4O_3$	*this study*
Bisu-07	302.2069	302.2080	3.640	$C_{14}H_{28}N_3O_4$	*this study*
Bisu-08	298.1394	298.1403	3.019	$C_{13}H_{20}N_3O_5$	*this study*
Bisu-09	293.1472	293.1461	3.752	$C_{10}H_{21}N_4O_6$	*this study*
Coelichelin					
Coelichelin	566.2769	566.2786	3.002	$C_{21}H_{40}N_7O_{11}$	8
Coeli-01	491.2468	491.2466	0.407	$C_{19}H_{35}N_6O_9$	*this study*
Nalidixic acid					
Nalidixic acid	233.0930	233.0926	1.716	$C_{12}H_{13}N_2O_3$	9

Table S4: Summary of database entries. Identified compounds with corresponding database IDs of the GNPS library. The newly isolated compound is highlighted by bold letters.

Name	Detected in supernatant	Analytic standard	Library ID
Calcimycin	x	x	CCMSLIB00003739947
***Cal-01* (deoxacalcimycin)**	x		CCMSLIB00003739953
N-demethyl-calcimycin	x		CCMSLIB00003739954
Cezomycin	x		CCMSLIB00003739955
Cal-02	x		CCMSLIB00003739956
Tuni-01 18:1	x		CCMSLIB00003739959
Tunicamycin D	x		CCMSLIB00003739960
Tuni-02 16:0	x		CCMSLIB00003739961
Tunicamycin B	x		CCMSLIB00003739962
Tunicamycin VI	x		CCMSLIB00003739963
Tunicamycin A	x		CCMSLIB00003739964
Tuni-03 14:0	x		CCMSLIB00003739965
Tuni-04 13:0	x		CCMSLIB00003739966
Tunicamycin I	x		CCMSLIB00003739967
Desf-01	x		CCMSLIB00003739969
Desferrioxamine G1	x		CCMSLIB00003739970
Desferrioxamine D1	x		CCMSLIB00003739971
Desferrioxamine E	x		CCMSLIB00003739972
Desf-02	x		CCMSLIB00003739973
Desferrioxamine D2	x		CCMSLIB00003739974
Desf-03	x		CCMSLIB00003739975
Desf-04	x		CCMSLIB00003739976
Desf-05	x		CCMSLIB00003739977
Desferrioxamine X1/7	x		CCMSLIB00003739978
Desferrioxamine B	x		CCMSLIB00003739979
Desferrioxamine A1	x		CCMSLIB00003739980
Desferrioxamine uA1	x		CCMSLIB00003739981
Desf-06	x		CCMSLIB00003739982
Desferrioxamine A2	x		CCMSLIB00003739983
Desf-07	x		CCMSLIB00003739984
Desf-08	x		CCMSLIB00003739985
Ferrioxamine H	x		CCMSLIB00003739986
Bisu-01	x		CCMSLIB00003739987
Bisu-02	x		CCMSLIB00003739988
Bisu-03	x		CCMSLIB00003739989
Bisucaberin	x		CCMSLIB00003739968
Bisu-04	x		CCMSLIB00003739990
dDFx[00-]	x		CCMSLIB00003739991
Bisu-05	x		CCMSLIB00003739992
Bisu-06	x		CCMSLIB00003739993
Bisu-07	x		CCMSLIB00003739994
Bisu-08	x		CCMSLIB00003739995
Bisu-09	x		CCMSLIB00003739996
Coelichelin	x		CCMSLIB00003739957
Coeli-01	x		CCMSLIB00003739958
Nalidixic acid	x	x	CCMSLIB00003739951
Ampicillin		x	CCMSLIB00003739946
Bacillibactin		x	CCMSLIB00003739997
Erythromycin		x	CCMSLIB00003739948
Erythromycin A Enol Ether		x	CCMSLIB00003739949
Monensin		x	CCMSLIB00003739950
Penicillin G		x	CCMSLIB00003739952
Tetracyclin		x	CCMSLIB00003739945

Table S5: Assigned ^{1}H (600 MHz) and ^{13}C (150 MHz) NMR data for deoxacalcimycin ($CDCl_3$).

position	δ_C, type	δ_H (*J* in Hz)	COSY[b]	HMBC[c]	NOESY[b]
1	170.0, C				
2	122.3, C				
3	123.3, CH	7.57, br d (7.8)	4	1, 5, 7	
4	126.5, CH	7.19, t (7.8)	3,5	2, 6	
5	125.6, CH	7.27-7.23, m	4	3, 7	
6	150.5, C				
7	127.5, C				
8-NH		10.40, br s			10a, 11
9	172.4, C				
10a	42.1, CH_2	2.69, dd (12.9, 8.1)	10b, 11	9, 11, 12	8-NH
10b		2.46, dd (12.9, 7.4)	10a, 11	9, 11, 12	
11	69.1, CH	3.94, app. td (7.8, 2.1)	10a, 10b, 12	9, 10, 13, 15, 27	8-NH
12	29.5, CH	1.42-1.36, m	27	13/14, 27	
13a	25.8, CH_2	1.26-1.18, m	13b, 14a	15, 27	
13b		1.09-1.03, m	13a	11	
14a	25.7, CH_2	1.73, app td (13.6, 4.6)	13a, 14b	12, 13, 15, 16	
14b		1.04-0.98, m	14a	15	
15	98.6, C				
16	32.7, CH	1.66-1.59, m	17a, 28	14, 15, 17, 18, 28	
17a	35.0, CH_2	1.84-1.77, m	16	15, 18	
17b		1.33-1.27, m		15, 16, 18, 19, 28, 29	
18	28.5, CH	1.84-1.77, m	19, 29		
19	73.6, CH	3.89, dd (10.2, 1.7)	18, 20	15, 17, 20, 21, 29, 30	
20	43.0, CH	3.24, dq (10.2, 6.9)	19, 30	18, 19, 21, 22, 30	23
21	196.0, C				
22	132.9, C				
23	119.6, CH	7.06-7.03, m	24	22, 24, 25	20
24	111.0, CH	6.28-6.25, m	23, 25	22, 23, 25	
25	126.8, CH	7.10-7.08, m	24	22, 23, 24	
26-NH		10.45, br s			
27	10.8, CH_3	0.88, d (6.6)	12	11, 12, 13	
28	16.4, CH_3	0.88, d (6.6)	16	15, 16, 17	
29	11.6, CH_3	0.99, d (7.0)	18	17, 18, 19	
30	12.9, CH_3	0.92, d (6.9)	20	19, 20, 21	

[a] δ in ppm relative to residual solvent signal of $CDCl_3$ (^{1}H: 7.26 ppm; ^{13}C: 77.16 ppm). [b] COSY and NOESY correlations are from the proton(s) stated to the indicated proton. [c] HMBC correlations are from the proton(s) stated to the indicated carbon.

Supplementary figures

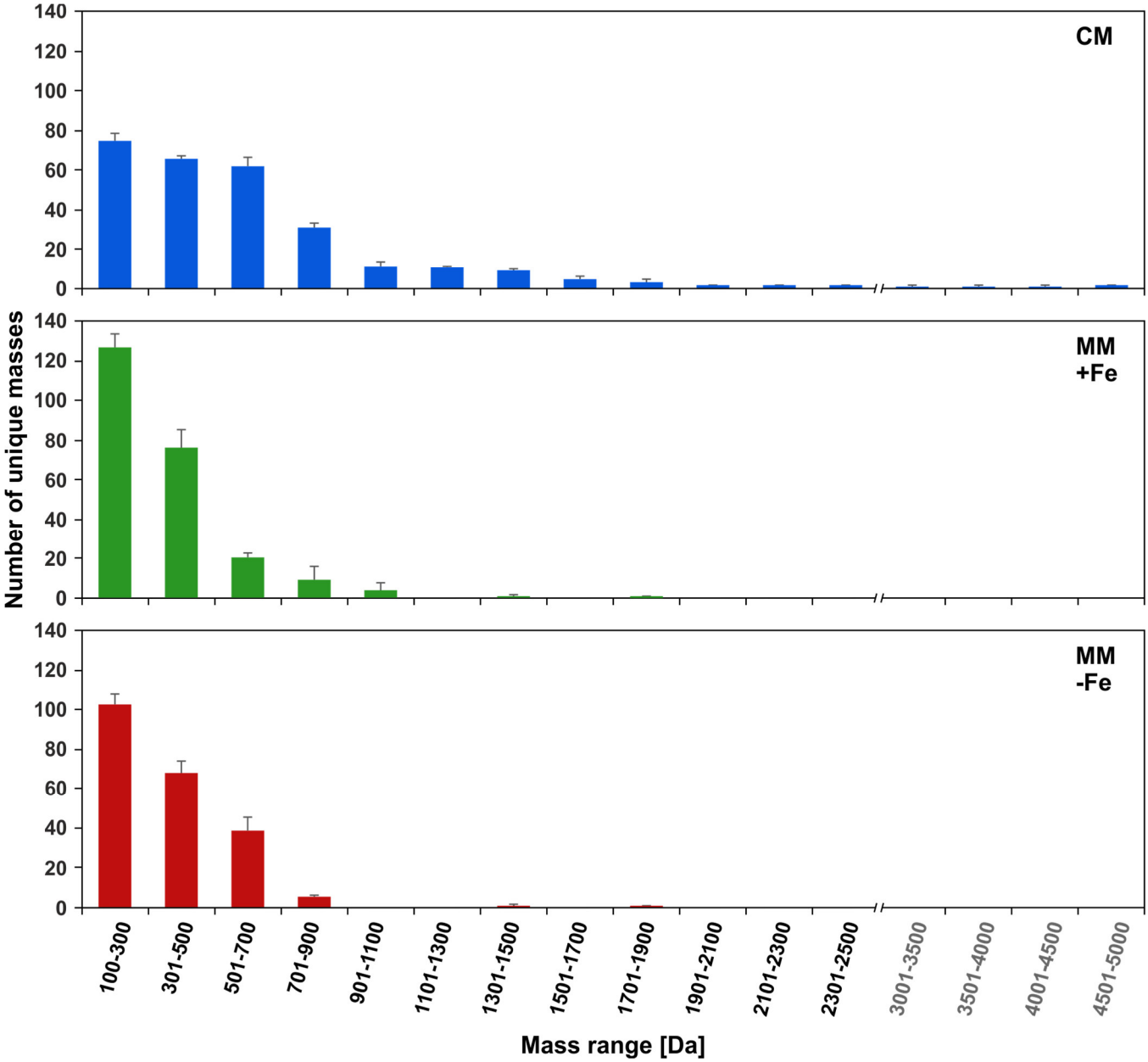

Figure S1: Unique metabolites of *S. chartreusis*. *S. chartreusis* produces unique and common metabolites when cultivated in complex medium (CM), minimal medium with (MM+Fe) and without (MM-Fe) iron. A sum of 701 unique parent masses was found under the tested cultivation conditions. No compounds were detected in the range of 2,501 to 3,000 Da. The experiment was performed in three independent biological replicates (*n*=3), and averages with standard deviations are shown. Data were processed as described in materials and methods section (charge corrected, dereplicated, adducts eliminated and background and medium components removed).

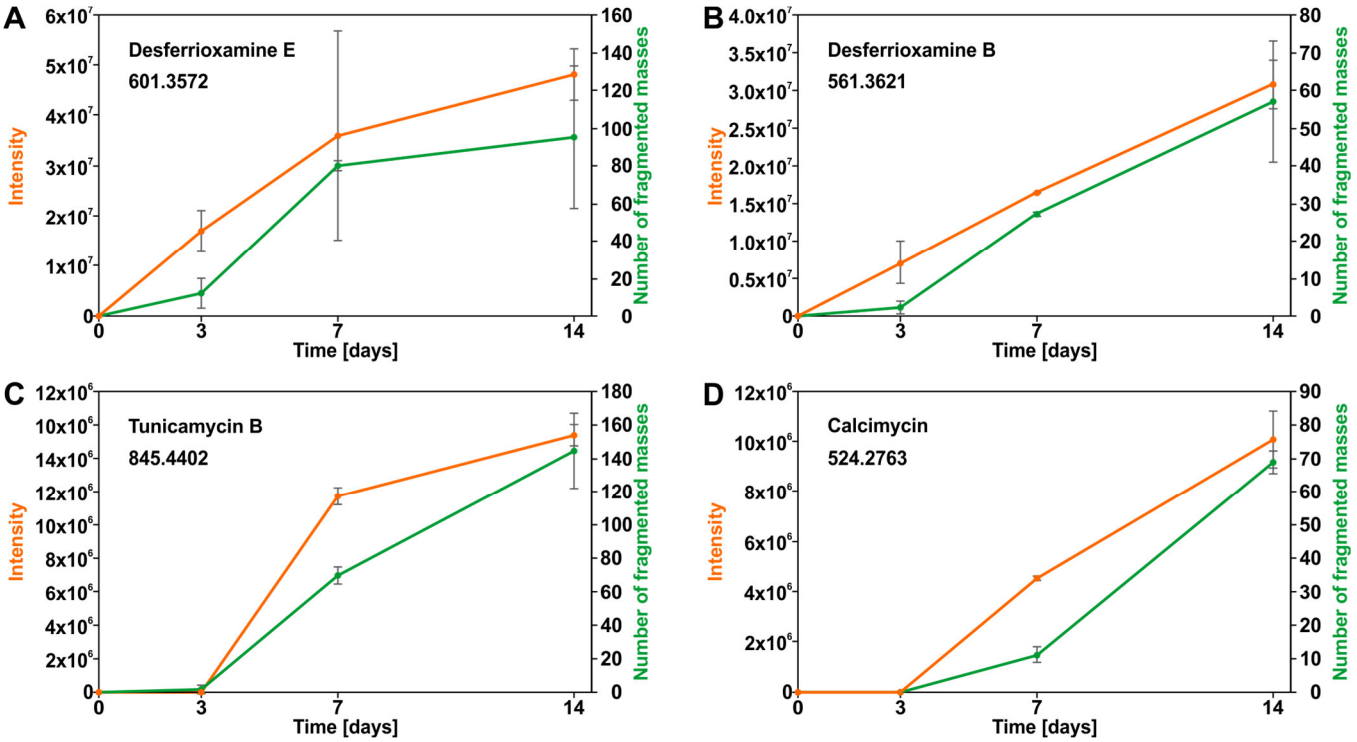

Figure S2: Comparison of quantitation by signal intensity and spectral counting. Exemplarily shown are the intensities and number of fragmented masses (spectral counts) of the siderophores desferrioxamine E and B, as well as the antibiotics calcimycin and tunicamycin B in complex medium (CM). The experiment was performed in three independent biological replicates (*n*=3), and averages with standard deviations are shown.

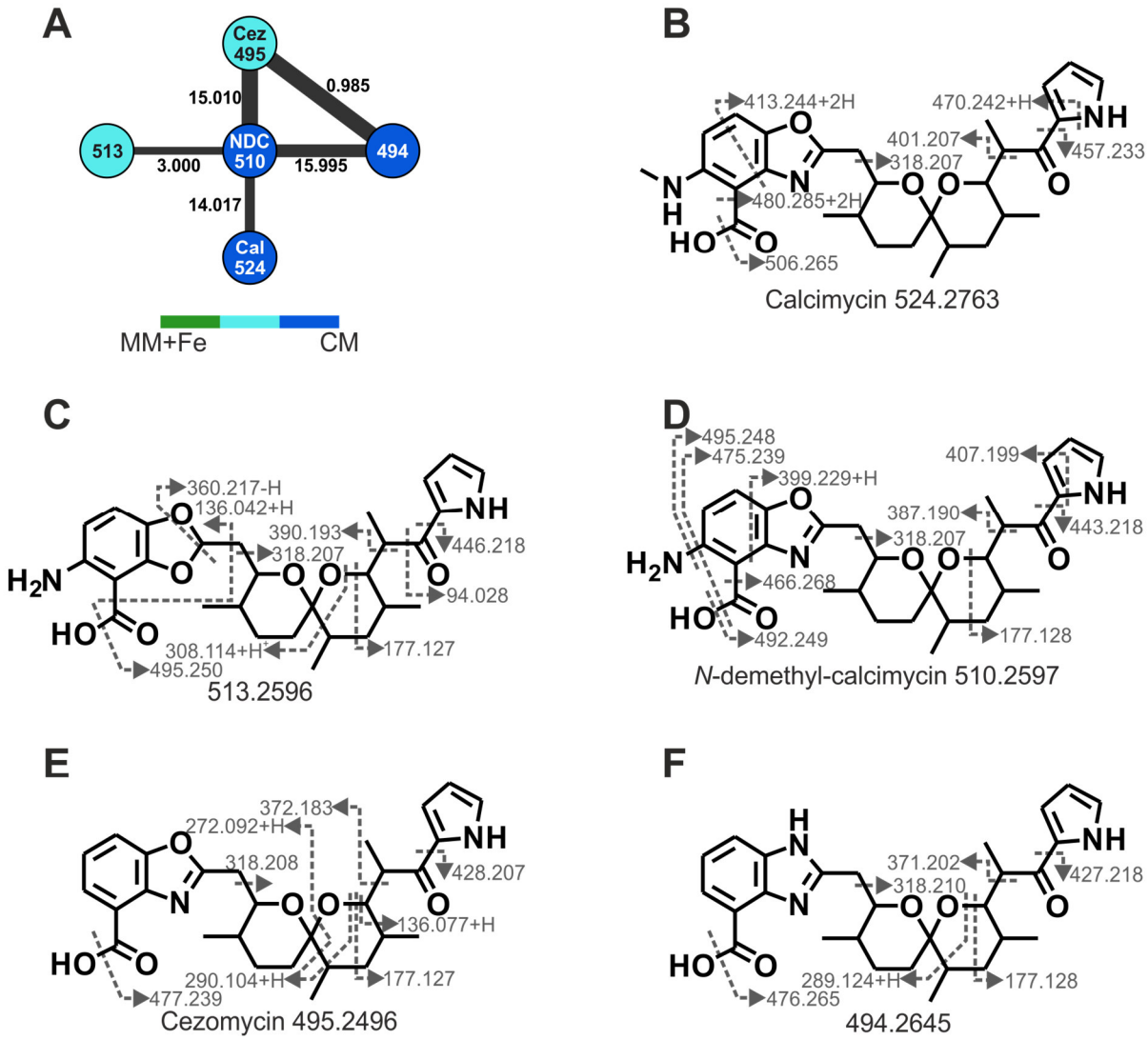

Figure S3: Calcimycin subnetwork, structures and fragments. (**A**) The molecular network of calcimycin. Molecules are represented by their protonated mass in Da and names of known variants. Colors indicate appearance in complex (CM, blue), minimal medium with iron (MM+Fe, green), or under both conditions (turquois). The thicknesses of connecting lines indicate the cosine similarity of fragmentation spectra, while the factors given describe the mass difference in Da. (**B-F**) Structure predicted based on LC-MS/MS data and annotation of fragment spectra of all calcimycin derivatives. The final structure of compound C was determined by NMR analysis of purified deoxacalcimycin and deviates from the predicted structure (see **Figure S10)**. Given are the masses of protonated molecules $[M+H]^+$ and the *m/z* of detected fragments. Grey lines indicate fragmentation sites, while light grey connects fragmentation sites.

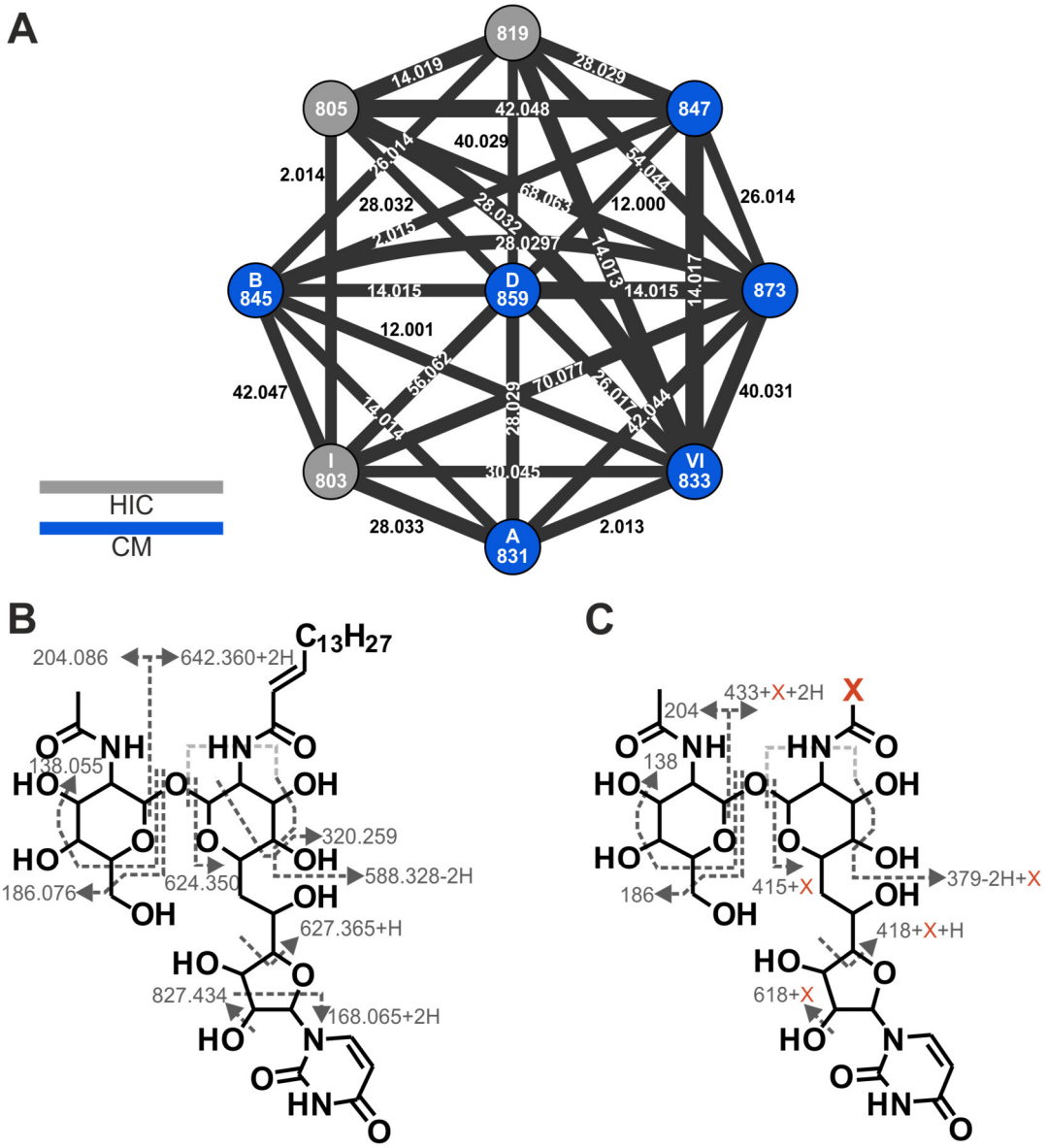

D

name	parent mass $[M+H]^+$	retention time [s]	X-chain composition	X-chain saturation
Tunicamycin 13:1 I	803.3934	1056.60	$C_{12}H_{23}$	unsaturated
Tunicamycin 13:0	805.4073	1063.93	$C_{12}H_{25}$	saturated
Tunicamycin 14:0	819.4261	1093.76	$C_{13}H_{27}$	saturated
Tunicamycin 15:1 A	831.4263	1117.77	$C_{14}H_{27}$	unsaturated
Tunicamycin 15:0 VI	833.4388	1124.05	$C_{14}H_{29}$	saturated
Tunicamycin 16:1 B	845.4402	1133.37	$C_{15}H_{29}$	unsaturated
Tunicamycin 16:0	847.4555	1180.90	$C_{15}H_{31}$	saturated
Tunicamycin 17:1 D	859.4554	1184.52	$C_{16}H_{31}$	unsaturated
Tunicamycin 18:1	873.4699	1260.47	$C_{17}H_{33}$	unsaturated

Figure S4: Tunicamycin subnetwork, structures, and fragments. (**A**) The molecular network of tunicamycin. Molecules are represented by their protonated mass in Da and names of known variants. Colors indicate appearance in complex medium (CM, blue), and in the hydrophobic interaction purification of minimal medium without iron (HIC, grey). The thicknesses of connecting lines indicate the cosine similarity of fragmentation spectra, while the factors given describe the mass difference in Da. (**B-D**) Structure prediction and annotation of fragment spectra of all tunicamycin derivatives. Given are the masses of protonated molecules $[M+H]^+$ and the *m/z* of detected fragments. Grey lines indicate fragmentation sites, while light grey connects fragmentation sites.

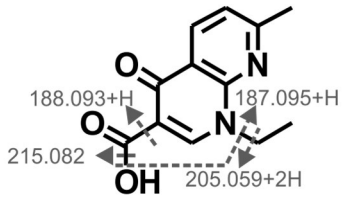

Nalidixic Acid 233.0930

Figure S5: Nalidixic acid. Annotation of the fragment spectrum of nalidixic acid. Given are the masses of protonated molecules $[M+H]^+$ and the *m/z* of detected fragments. Grey lines indicate fragmentation sites.

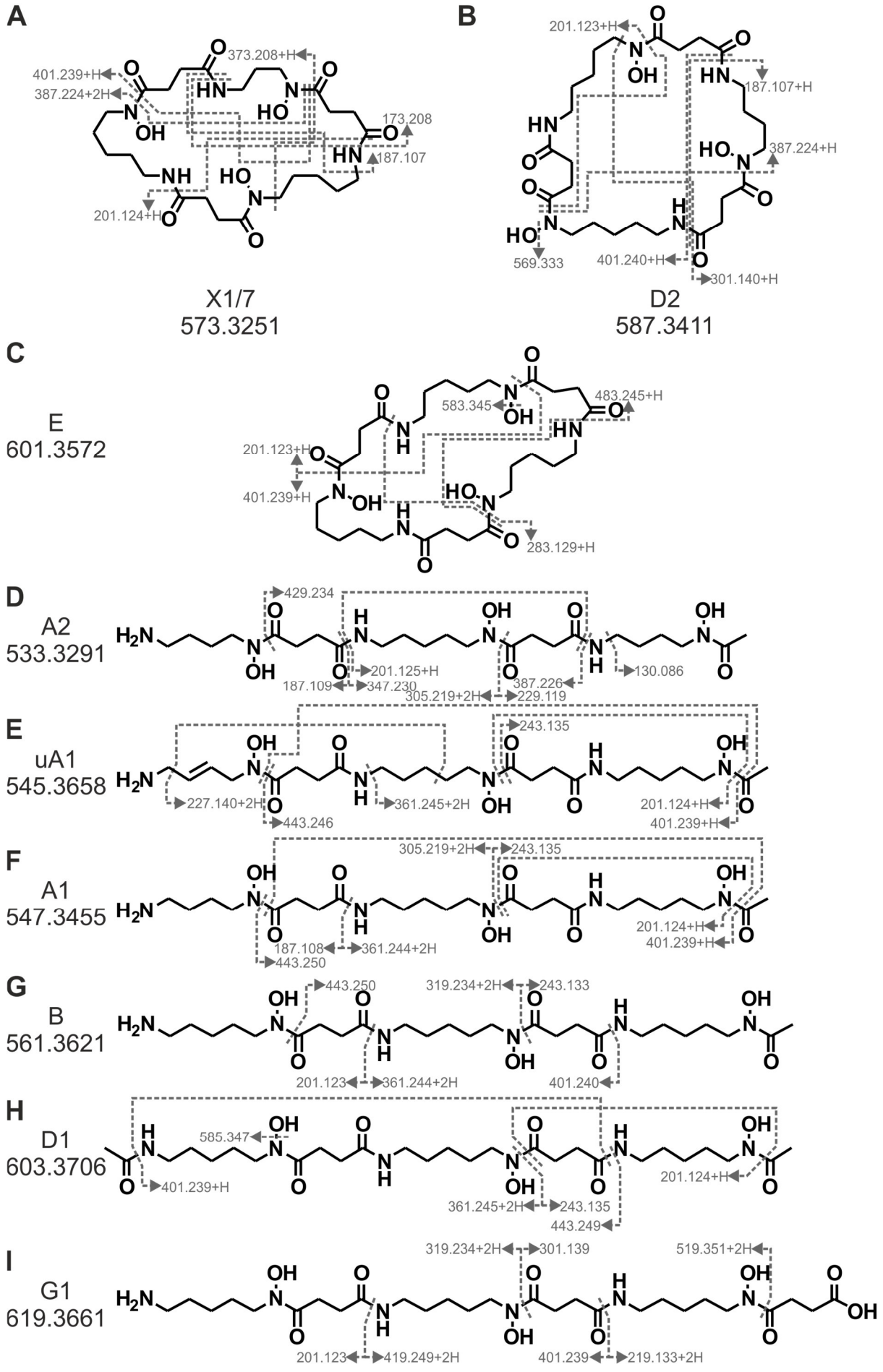

Figure S6: Desferrioxamine subnetwork, structures, and fragments of known compounds. Annotation of fragment spectra of all known desferrioxamine siderophores detected in this study. Given are the denotations, masses of protonated molecules $[M+H]^+$, and the *m/z* of detected fragments. Grey lines indicate fragmentation sites, while light grey connects fragmentation sites.

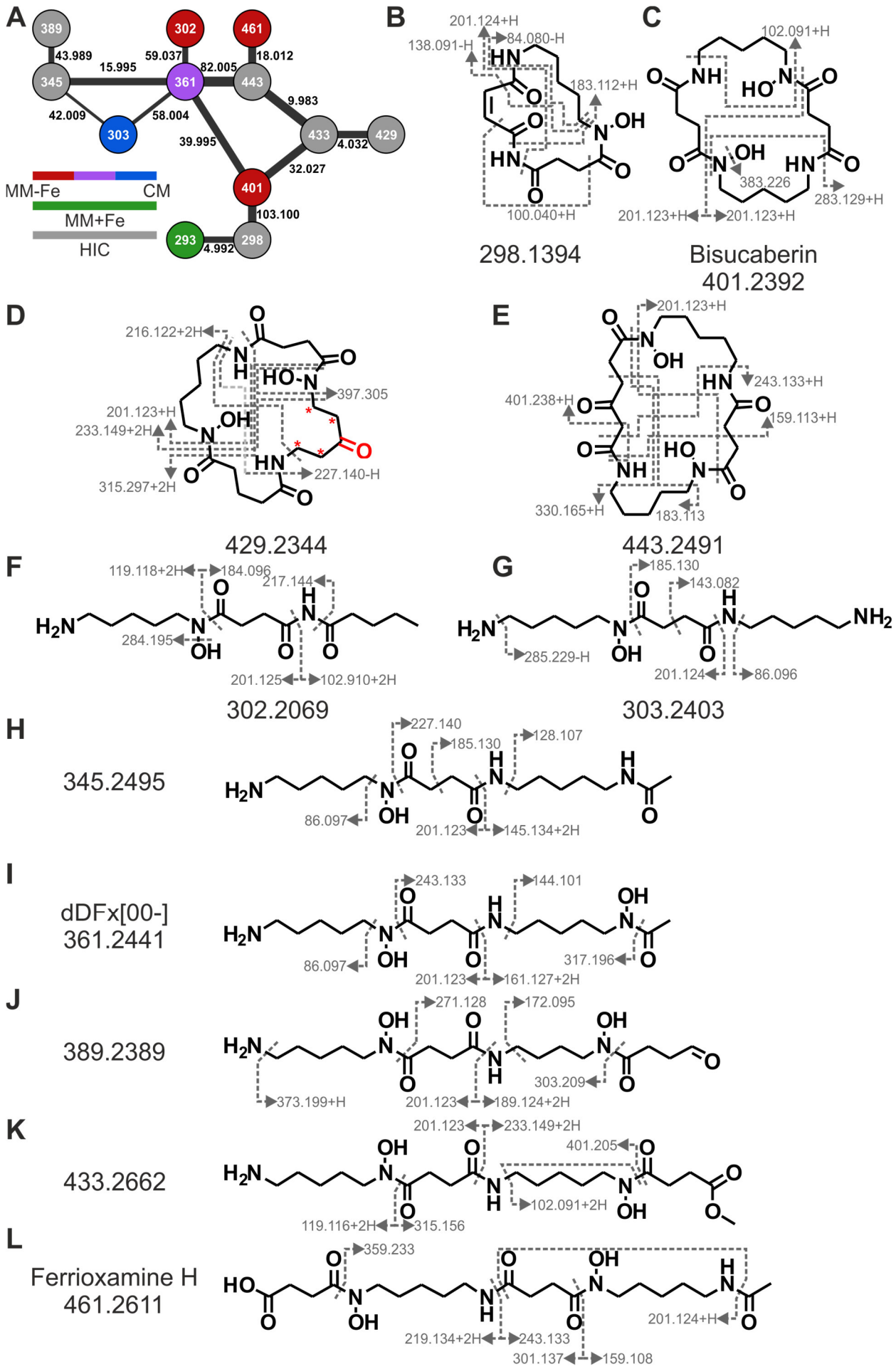

Figure S7: Bisucaberin subnetwork, structures, and fragments. (**A**) The molecular network of bisucaberin. Molecules are represented by their protonated mass in Da and names of known variants. Colors indicate appearance in complex (CM, blue), minimal medium without iron (MM-Fe, red), under both conditions (purple), in minimal medium with iron (MM+Fe, green), and in a hydrophobic interaction purification of minimal medium without iron (HIC, grey). The

thicknesses of connecting lines indicate the cosine similarity of fragmentation spectra, while the factors given describe the mass difference in Da. (**B-L**) Structure prediction and annotation of fragment spectra of bisucaberin derivatives. Given are the masses of protonated molecules $[M+H]^+$ and the *m/z* of detected fragments. The red asterisk (*) shows potential positions of red marked oxygen. Grey lines indicate fragmentation sites, while light grey connects fragmentation sites. No structure was predicted for compound 293.

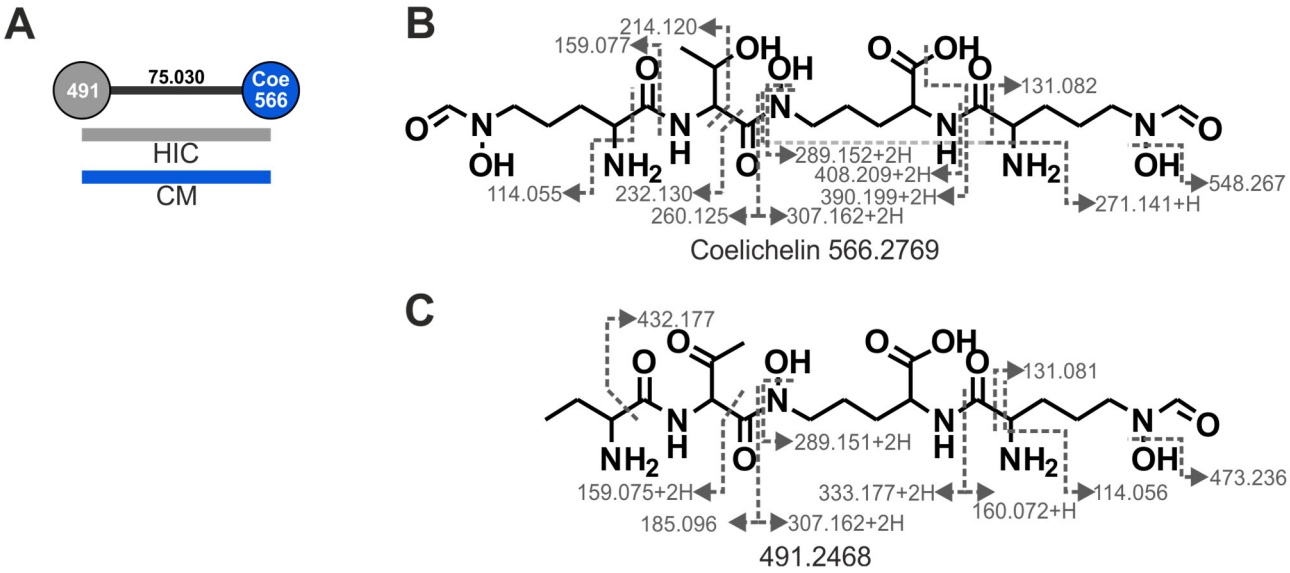

Figure S8: Coelichelin subnetwork, structures and fragments. (**A**) The molecular network of coelichelin. Molecules are represented by their protonated mass in Da and names of known variants. Colors indicate appearance in complex medium (CM, blue) and in a hydrophobic interaction purification of minimal medium without iron (HIC, grey). The thicknesses of connecting lines indicate the cosine similarity of fragmentation spectra, while the factors given describe the mass difference in Da. (**B, C**) Structure prediction and annotation of fragment spectra of all coelichelin derivatives. Given are the masses of protonated molecules $[M+H]^+$ and the *m/z* of detected fragments. Grey lines indicate fragmentation sites, while light grey connects fragmentation sites.

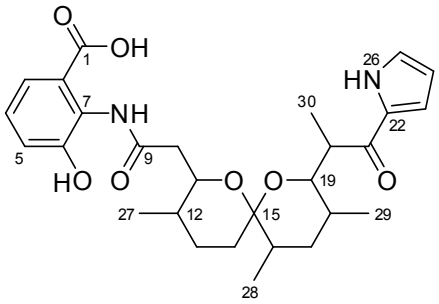

Figure S9: Chemical structure of deoxacalcimycin. $[\alpha]^{25}_D$ = -82.5 (*c* 0.1983 in $CHCl_3$); IR ν_{max} 3271, 2964, 2933, 1692, 1638, 1545, 1465, 1431, 1408, 1386, 1374, 1276, 1239, 1197, 1137, 1078, 989, 940, 917, 889, 858, 815, 756 cm^{-1}. HRESIMS *m/z* 513.2594 $[M+H]^+$ (calcd for $C_{28}H_{37}N_2O_7$, 513.2595). ESI-MS/MS (CID, *m/z* 513.25 $[M+H]^+$): *m/z* 495.24 ($[M+H-H_2O]^+$), 477.23 ($[M+H-H_4O_2]^+$), 446.21 (b), 428.20 (b–H_2O), 360.21 (a), 342.20 (a–H_2O), 318.20, 293.17 (ab), 275.16 (ab–H_2O).

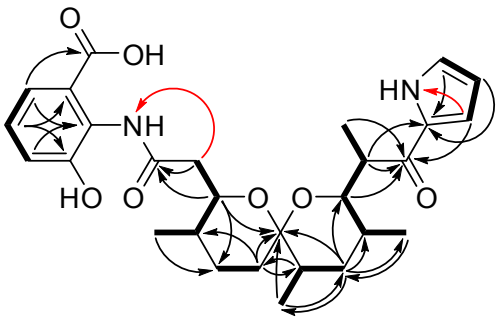

Figure S10: Selected COSY (bold bonds) and HMBC correlations (black: $^{1}H \rightarrow {}^{13}C$; red: $^{1}H \rightarrow {}^{15}N$) of deoxacalcimycin.

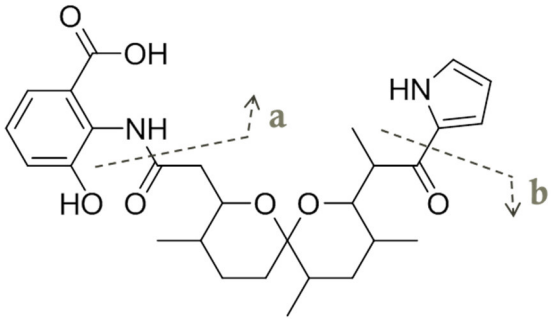

Figure S11: Proposed ESI-MS/MS fragmentation of deoxacalcimycin.

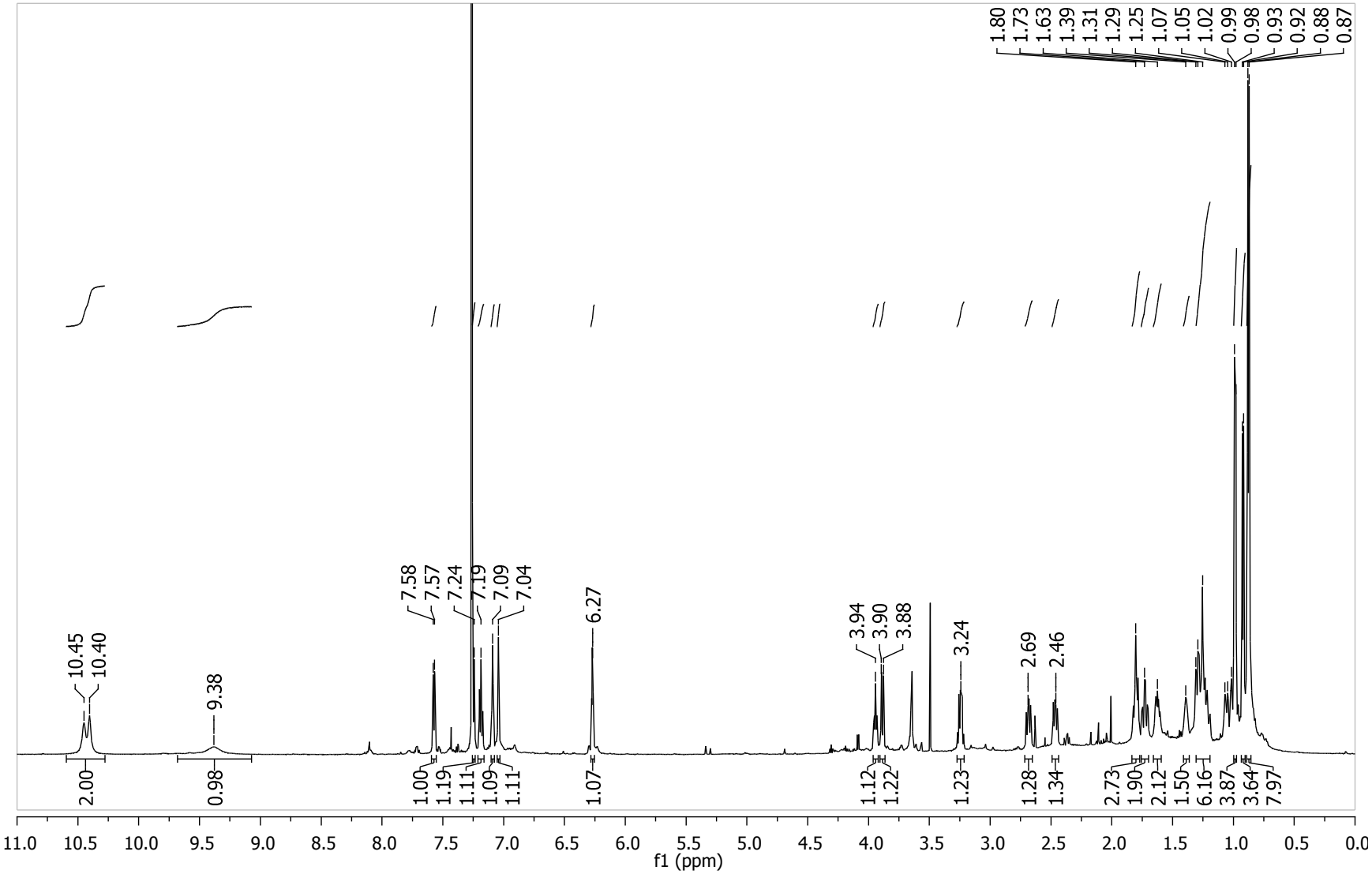

Figure S12: ^{1}H NMR spectrum (600 MHz) of deoxacalcimycin.

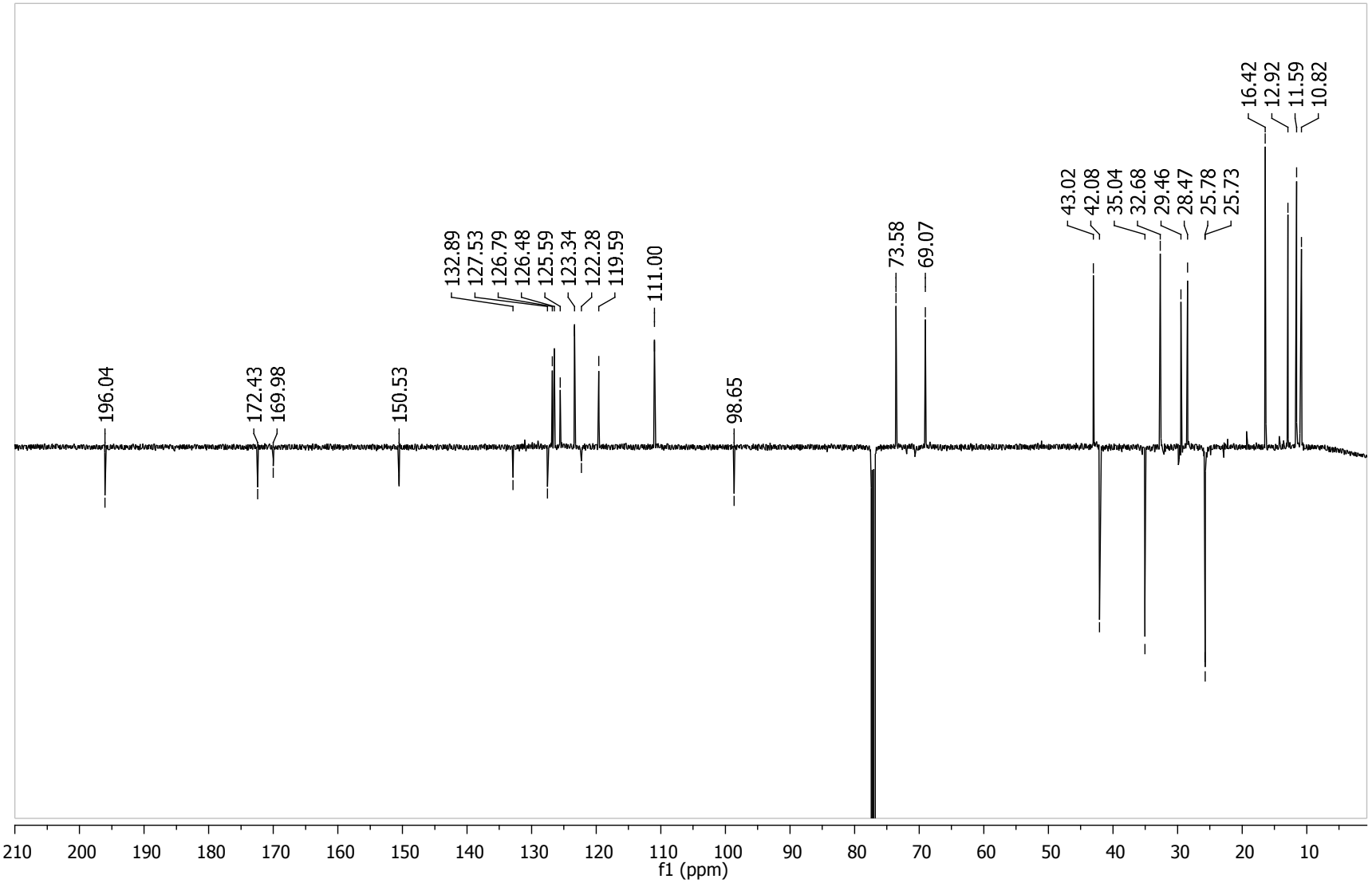

Figure S13: ^{13}C NMR spectrum (150 MHz) of deoxacalcimycin.

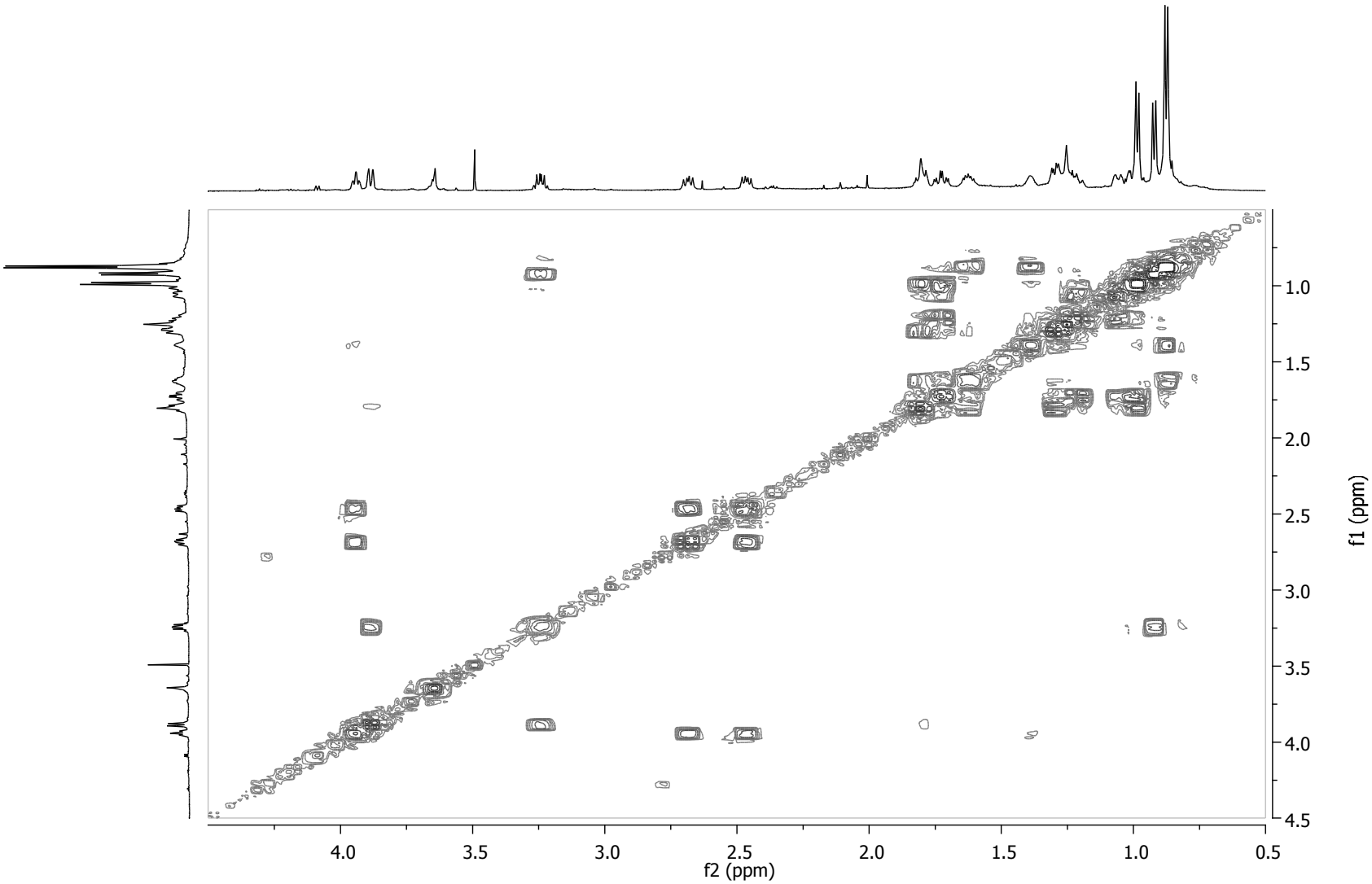

Figure S14: COSY spectrum (0.5-4.5 ppm) of deoxacalcimycin.

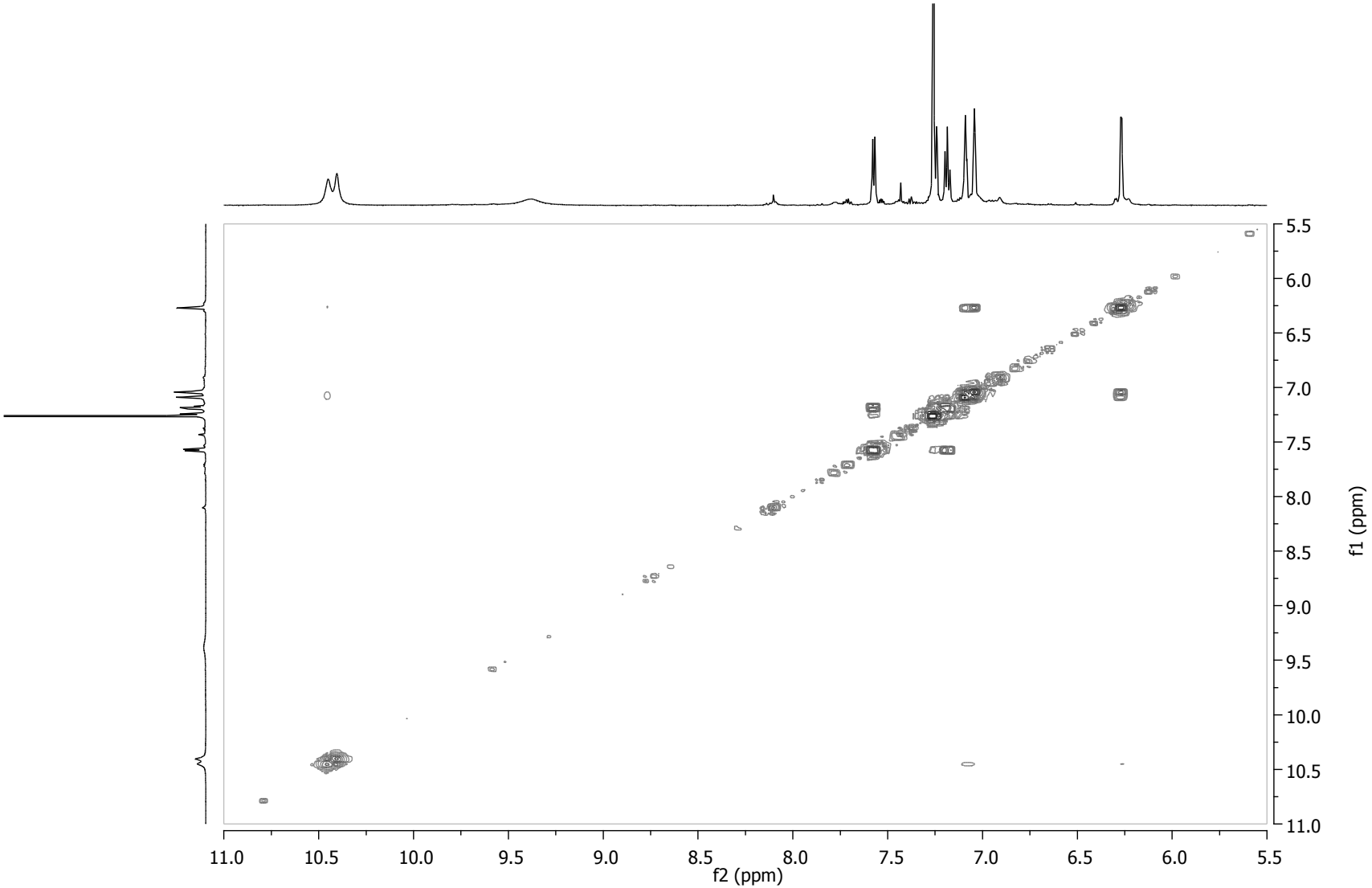

Figure S15: COSY spectrum (5.5-11.0 ppm) of deoxacalcimycin.

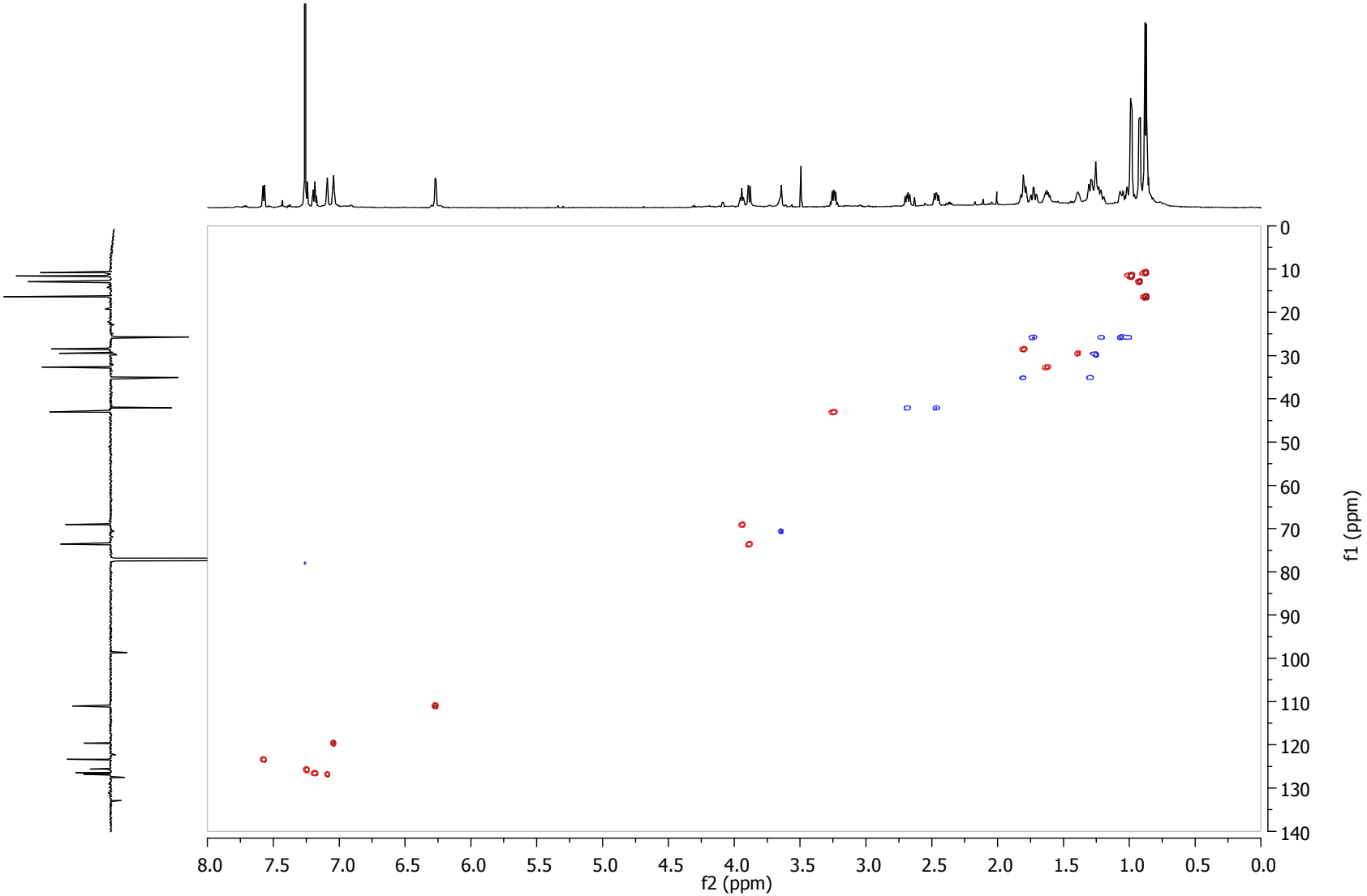

Figure S16: HSQC spectrum of deoxacalcimycin.

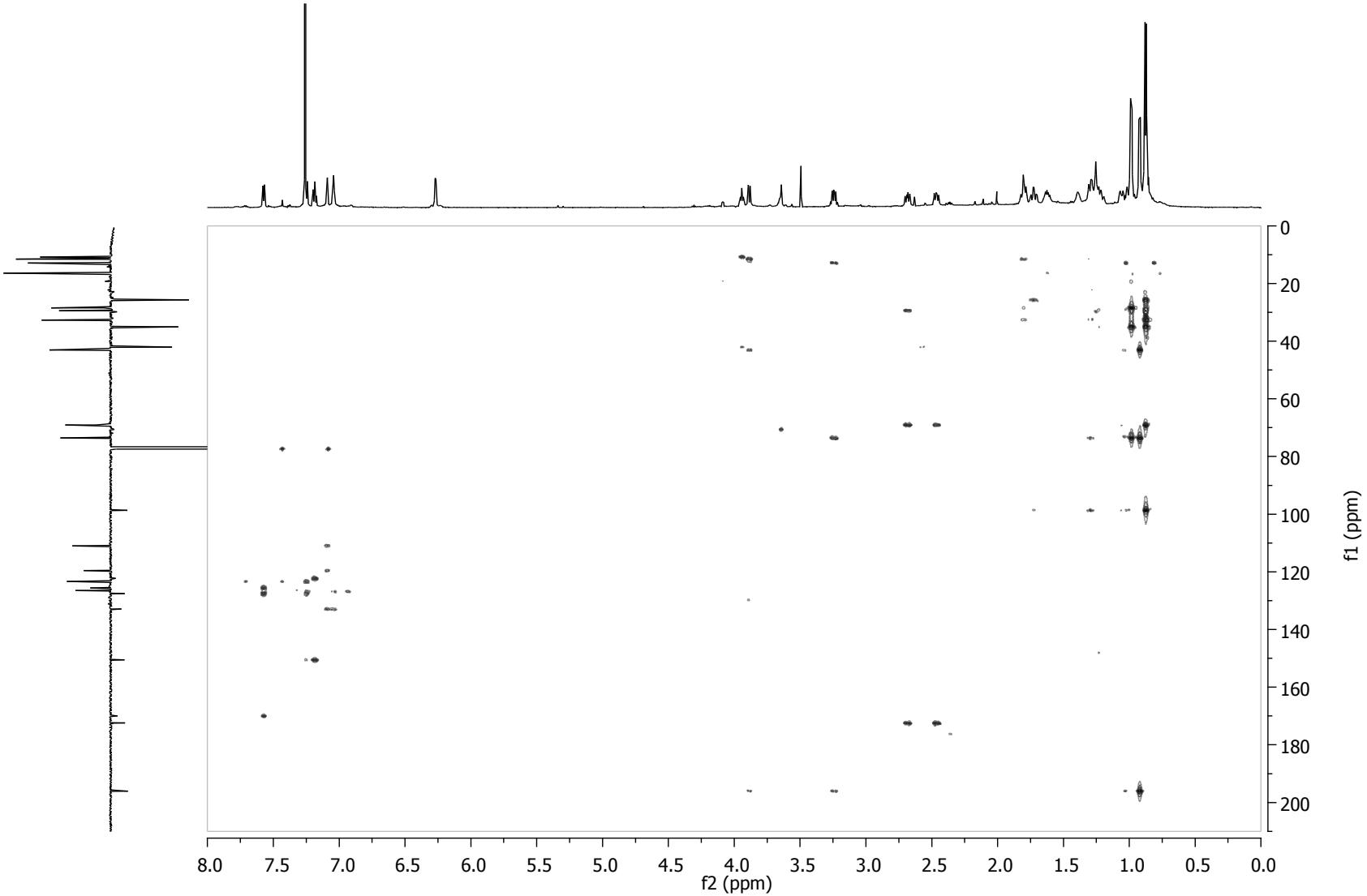

Figure S17: HMBC spectrum of deoxacalcimycin.

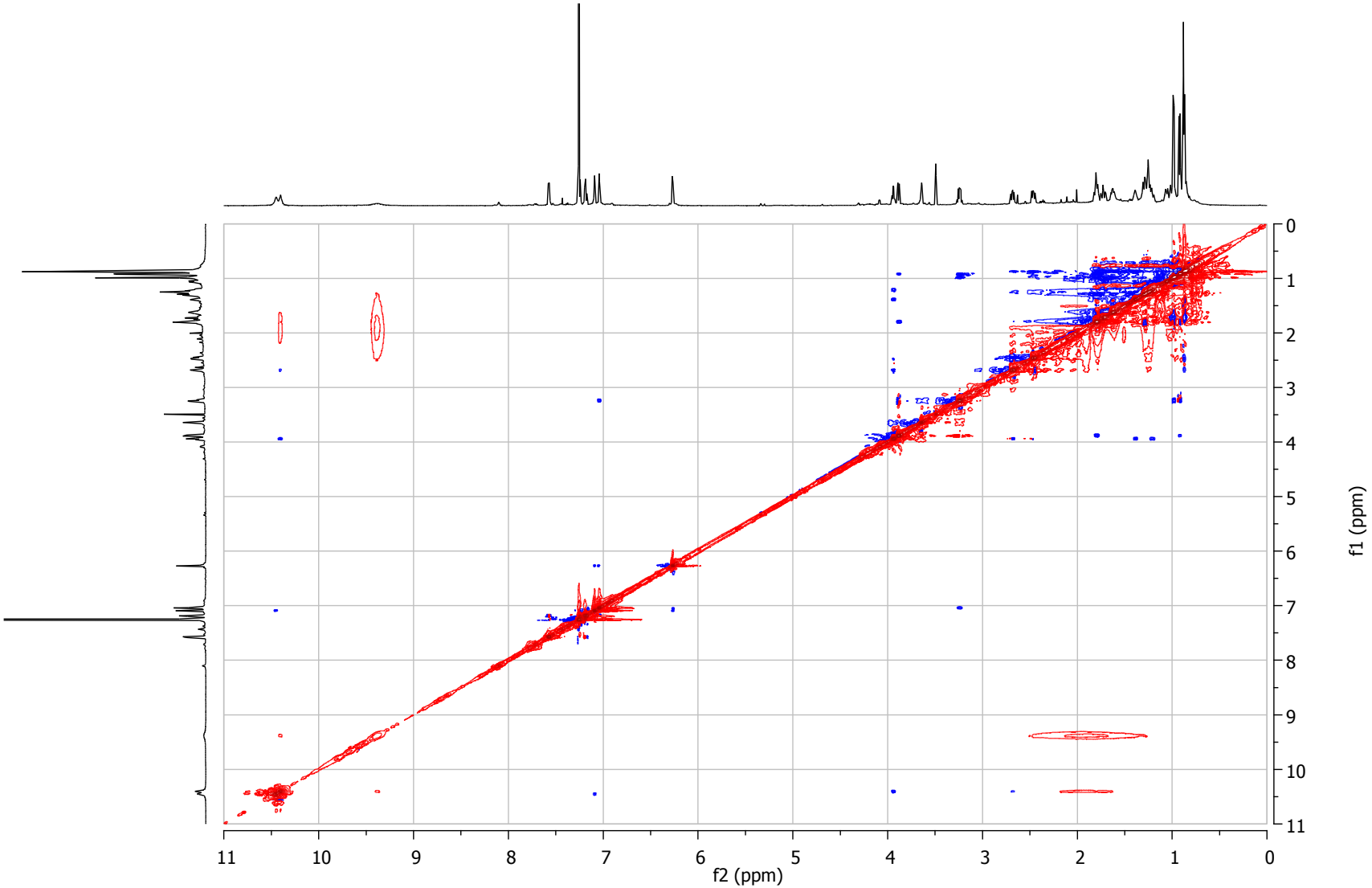

Figure S18: NOESY spectrum of deoxacalcimycin.

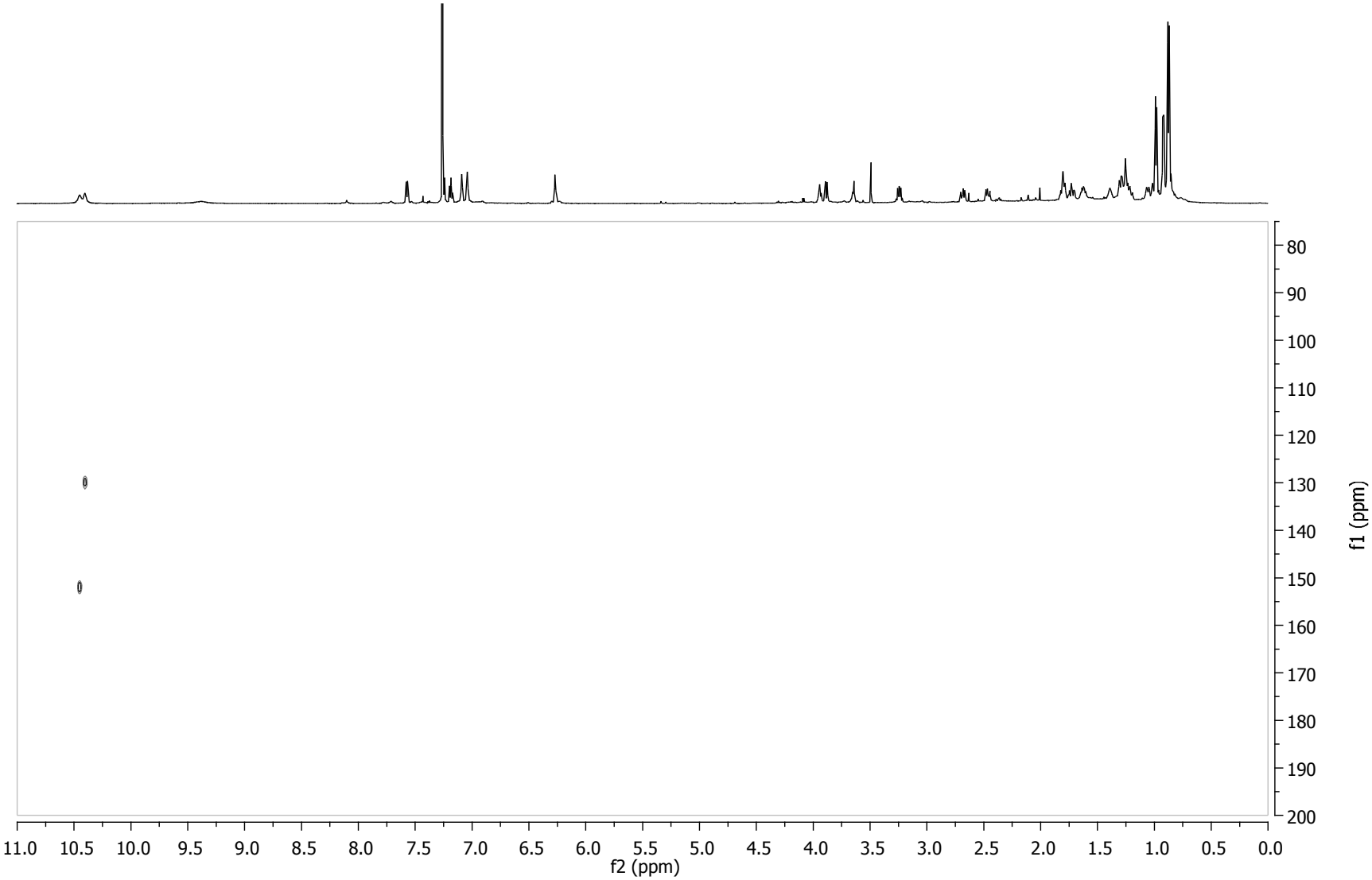

Figure S19: $^{1}H/^{15}N$ HSQC spectrum of deoxacalcimycin.

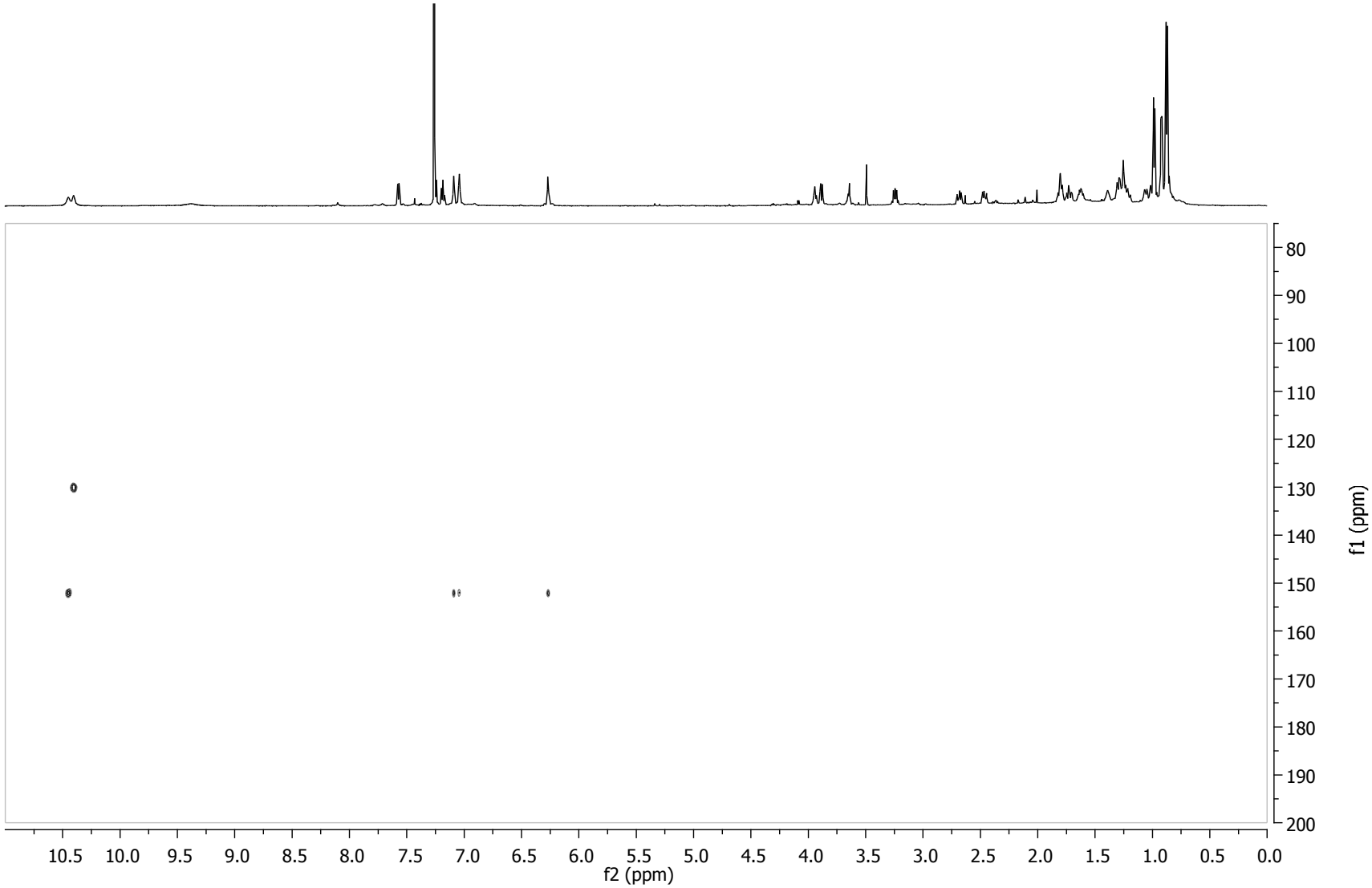

Figure S20: $^{1}H/^{15}N$ TOCSY-HSQC spectrum of deoxacalcimycin.

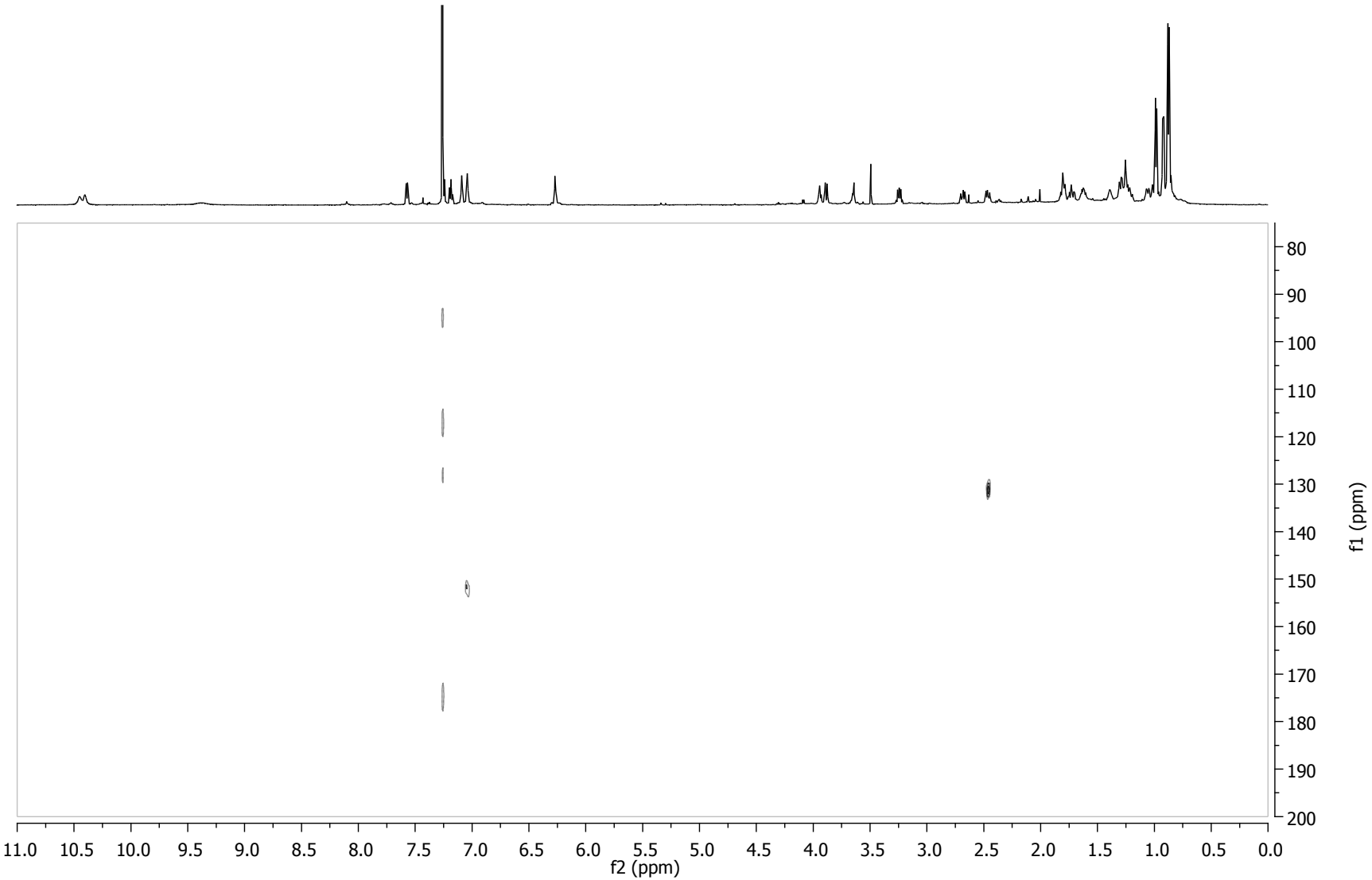

Figure S21: $^{1}H/^{15}N$ HMBC spectrum of deoxacalcimycin.

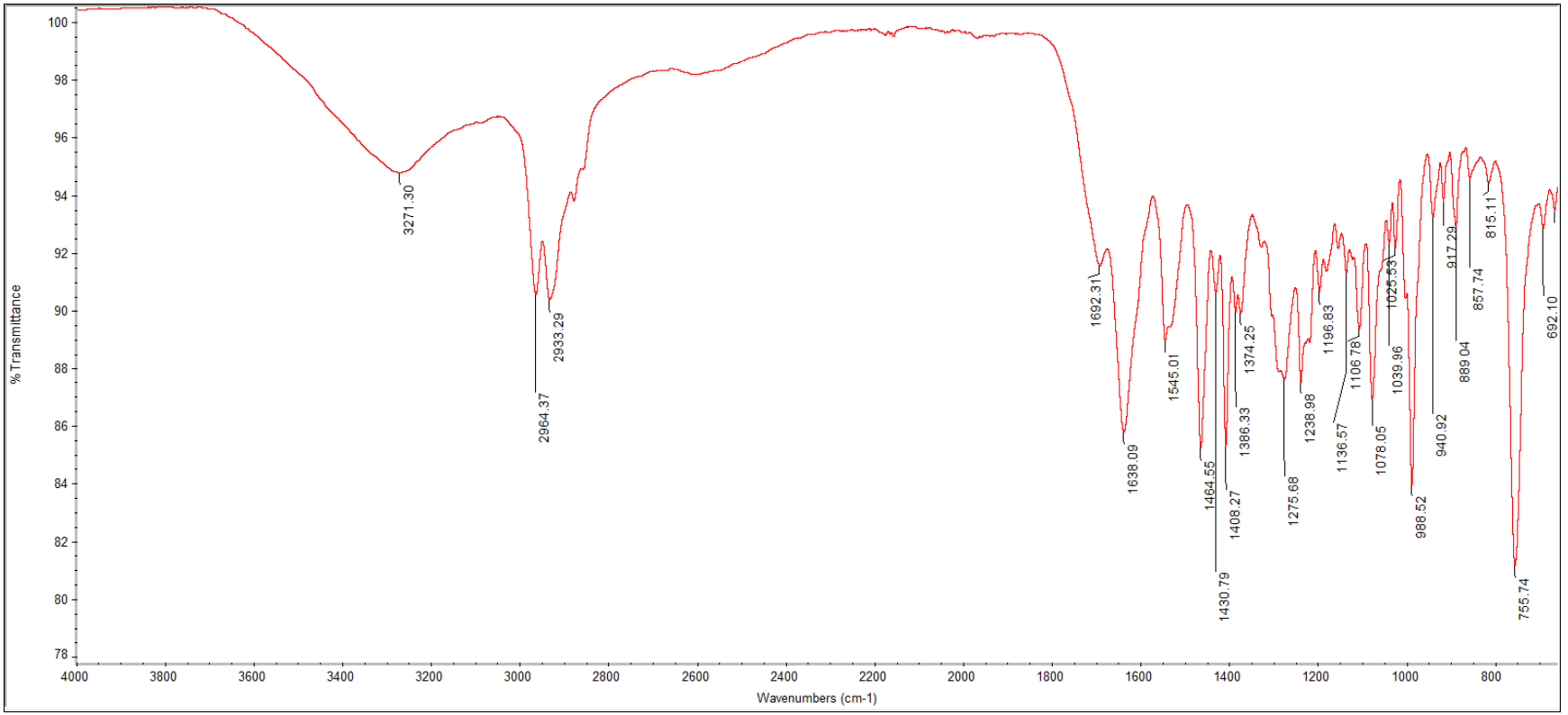

Figure S22: FTIR spectrum of deoxacalcimycin.

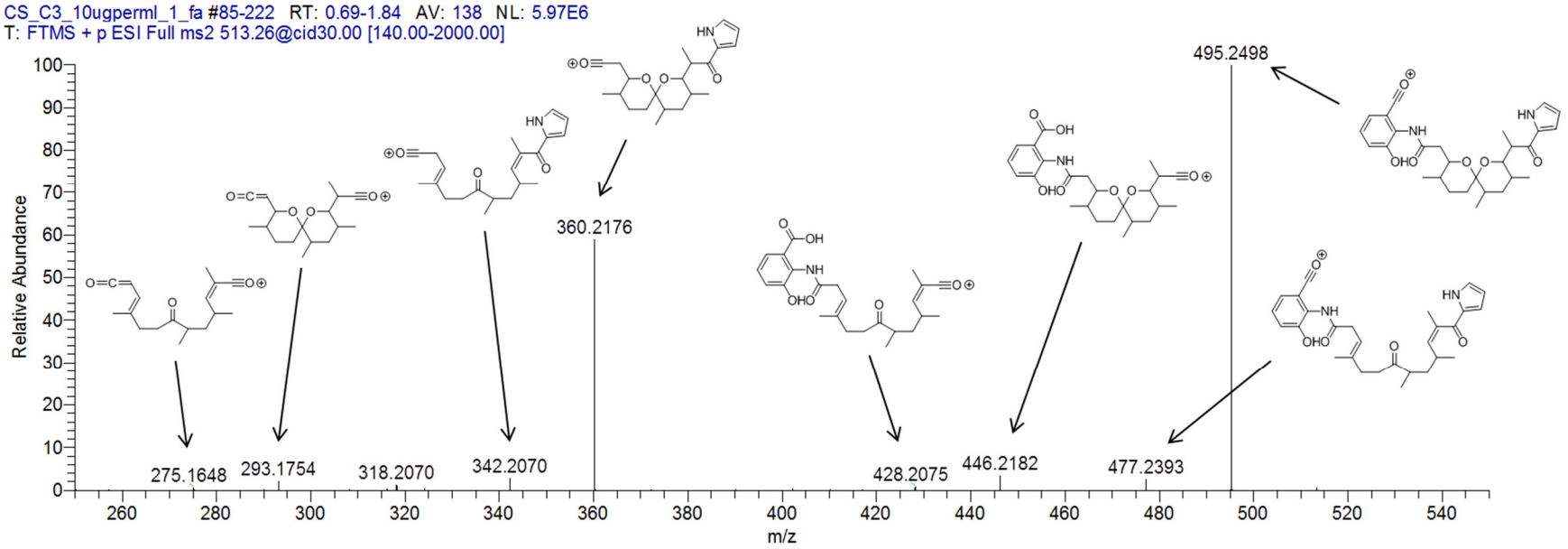

Figure S23: ESI-MS/MS spectrum of purified deoxacalcimycin and annotation of detected fragments.

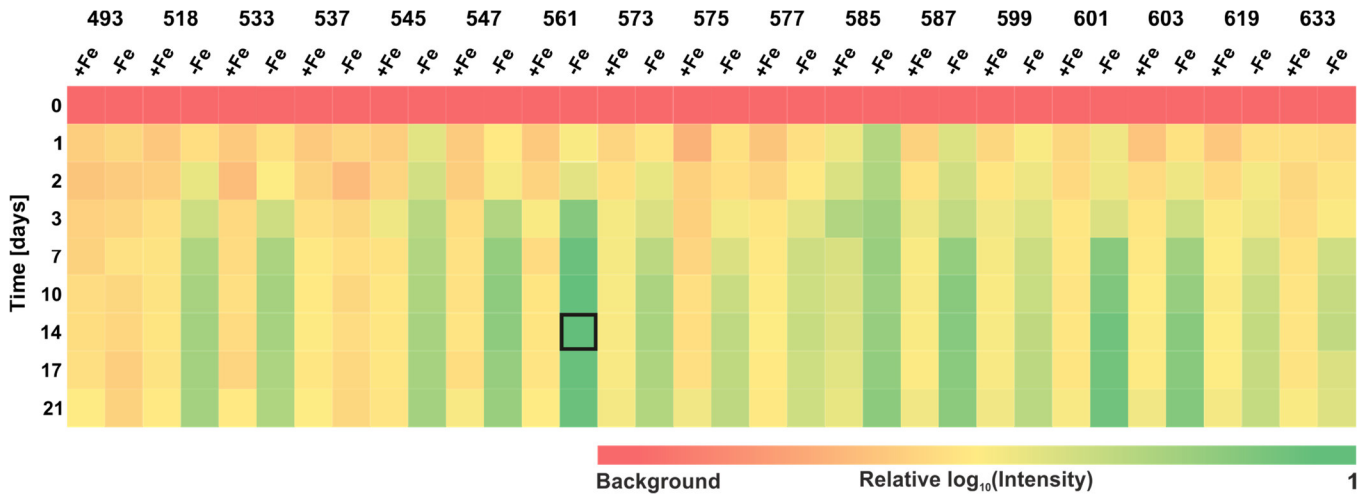

Figure S24: Siderophore production in minimal media. Given are the average $\log_{10}$ intensities of desferrioxamine siderophores (indicated by $[M+H]^+$) detected in three biological replicates of *S. chartreusis* cultivation in minimal medium with (+Fe) and without iron (-Fe). Intensities are related to the most intense signal (black frame). Further information on siderophore identity is provided in **Tab. S2**, **Fig. 3,** and **Fig. S6**.

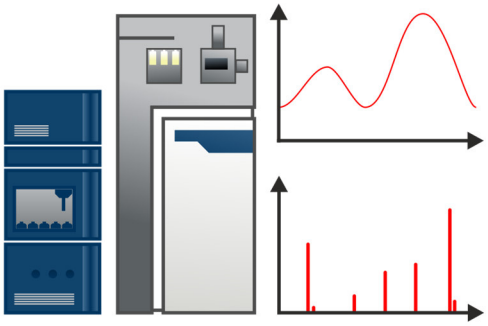

1. Collecting data.
By LC-MS/MS, for every detected compound information on the polarity (retention time), molecular formula (parent mass), and molecular structure (fragment spectrum) is gathered.

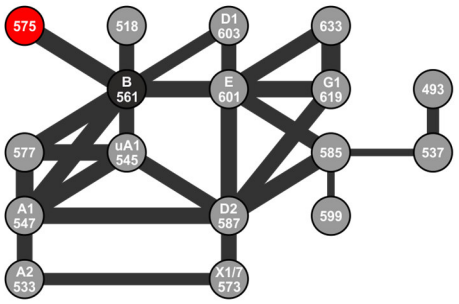

2. Generation of a molecular network.
Using the Global Natural Products Social Molecular Networking-platform (gnps.ucsd.edu) a molecular network based on the fragmentation spectra is generated. Compounds, represented by nodes in the network, are sorted based on the similarity of their fragmentation spectra. Nodes representing highly similar spectra are connected by edges and are likely to be structurally similar.

3. Annotation of fragment spectra for known compounds.
For identified compounds with known structures (B 561; black in 2.), for example identified by library searches or by comparison to standards, the signals in the fragment spectrum are assigned to the corresponding molecular fragments. This step can be aided by utilizing *in silico* fragmentation tools like MetFrag (msbi.ipb-halle.de/MetFrag/).

561.3621

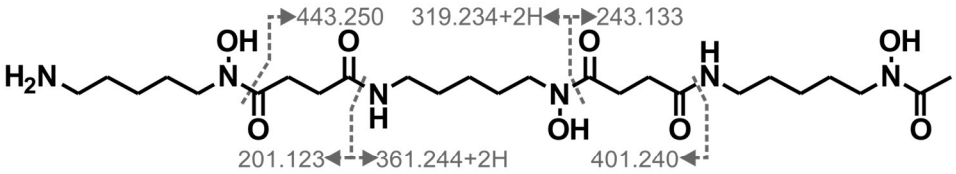

Formula	Monoisotopic Mass	Δppm
$C_{26}H_{51}N_6O_8$	575.3763	0.2
$C_{25}H_{55}N_2O_{12}$	575.3750	2.2
$C_{23}H_{42}N_{16}O_2$	575.3749	2.2
$C_{38}H_{46}N_4O$	575.3744	3.1
$C_{22}H_{46}N_{12}O_6$	575.3736	4.5

4. Prediction of the molecular formula.
Based on the parent mass the molecular formula of novel compounds (575; red in 2.) is predicted with tools like mMass (mmass.org). Through comparison with known derivatives, identified by molecular networking, the number of candidate formulae can be reduced by exclusion of unlikely compositions.

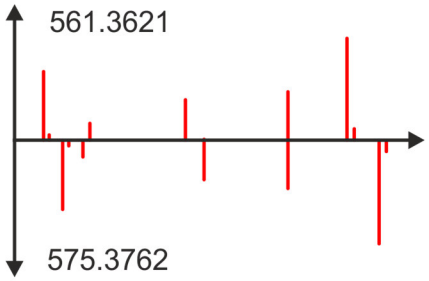

5. Comparison of fragment spectra.
Through comparison with annotated spectra of known compounds common molecular substructures as well as differences can be identified.

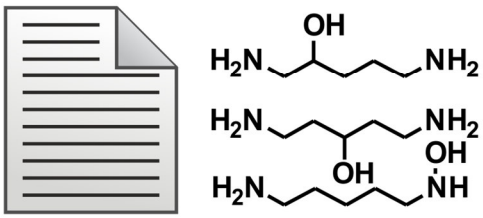

6. Structure prediction
Utilizing the molecular formulae and the information on common and unique fragments, a library of molecular structures is generated containing all possible variants of the candidate compound. Fragments are assigned to identify the structure. This process can again be aided by *in silico* fragmentation tools like MetFrag.

575.3762

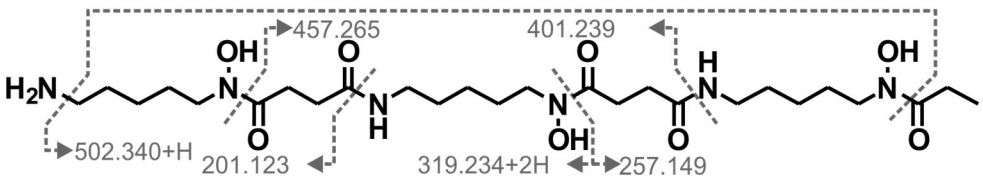

Figure S25: Basic workflow for networking-guided structure elucidation via tandem mass spectrometry. Desferrioxamine B (561) and desferrioxamine 575 serve as examples for the identification of known compounds and structural annotation of new compounds, respectively.

Methods

Strains and cultivation conditions. *Streptomyces chartreusis* NRRL 3882 was grown in YEME complex medium (CM), containing 3 g/l yeast extract, 5 g/l peptone, 3 g/l malt extract, 55.5 mM glucose, and 73 mM saccharose (10). NCBMM was used as a defined minimal medium (MM). NCBMM is a modified variant of Belitzky minimal medium (11) in which trisodium citrate was replaced by 21 mM NaCl, also containing 15 mM $(NH_4)_2SO_4$, 8 mM $MgSO_4$, 27 mM KCl, 50 mM Tris, 0,6 mM KH_2PO_4, 2 mM $CaCl_2$, 0.01 mM $MnSO_4$, 4.5 mM L-glutamate, 0.78 mM L-tryptophan, and 11 mM D-glucose. The pH was adjusted to 7.5 using HCl. Iron was added/omitted as 0.001 mM $FeSO_4$ when necessary. For compound purification ISP2 medium was used, containing 4 g/l yeast extract, 10 g/l malt extract, and 4 g/l glucose (12). *S. chartreusis* NRRL 3882 was cultivated at 30 °C and 180 rpm in an Innova orbital shaker.

DNA isolation and sequencing. DNA of *S. chartreusis* NRRL 3882 was isolated as described in Schwientek *et al.,* 2011 and Kieser *et al.,* 2000 (10, 13). In brief, *S. chartreusis* NRRL 3882 was cultivated in 10 ml YEME with 0.5% glycin for 48 h. Mycelia were harvested in 2 ml aliquots and washed in 500 µl 10% sucrose and subsequently 500 µl TE buffer (10 mM Tris, 5 mM EDTA, pH 8). Cells were disrupted in 300 µl TE buffer with 5 mg/ml lysozyme and 0.075 mg/ml pre-boiled RNAse A at 37 °C for 2 h. Afterwards 50 µl 5 M NaCl and 120 µl 10% SDS were added, the samples were boiled and 240 µl 5 M ice-cold potassium acetate was added prior to incubation at -20 °C. The DNA was pelleted with 600 µl ice-cold isopropanol, washed in 500 µl 70% ethanol, and solved in 30 µl of sterile H_2O. Final DNA concentrations were about 3800 ng/µl. In order to avoid problems with GC-rich regions, a whole-genome-shotgun PCRfree library (Nextera DNA Sample Prep Kit; Illumina, Munich, Germany) was generated for *S. chartreusis* NRRL 3882 based on the manufacturer's protocol. The resulting library was sequenced on the Illumina MiSeq platform. After sequencing and raw data processing with an in-house platform (14), a *de novo* assembly was obtained by applying the gsAssembler 2.8 (Roche) with default settings. For the annotation of the genome, the platforms Prokka 1.11 (15) and GenDB 2.0 (16) were applied.

AntiSMASH analysis. The complete genome was analyzed using the antibiotics & Secondary Metabolite Analysis Shell (antiSMASH version 3.0.5 (17)) with default settings.

Hydrophobic interaction chromatography. After 14 days of cultivation the culture supernatant of a 100 ml NCBMM-Fe culture was incubated with 25 mg/ml of Diaion HP-20 resin (Sigma-Aldrich) for three hours (18). The resin was washed with water and poured into a column. Elution was performed using three column volumes with 25%, 50%, and 100% CH_3OH subsequently.

LC-coupled MS/MS-measurements. Experiments were performed in three biological replicates. *S. chartreusis* was cultivated for 14 days in YEME and NCBMM+/-Fe. Culture supernatant was harvested after 0, 1, 3, 7, and 14 days. The supernatant (400 µl) was extracted with 1320 µl ethyl acetate. The aqueous phase was washed twice with 200 µl ethyl acetate and the organic phase with 200 µl water. Organic and aqueous phase were reduced *in vacuo* and reconstituted in 100 µl MS-grade CH_3OH.

Separation was performed by using a nanoACQUITY-UPLC system (Waters) with a Mixer Assy (Waters, zirc bead, inner cross section 1mm, length 50 mm) and an AcquityUPLC CSH C18 column (Waters, pore size 130 Å, particle size 1.7 µm, inner cross section dimension 1 mm, length 100 mm) and a H_2O/acetonitrile gradient with 0.1% formic acid (FA). The flow rate was 5 µl/min. The following gradient was used.

Gradient for LC-MS/MS

Time [min]	% ACN with 0.1% FA
Initial	5.0
5	5.0
18	99.5
29	99.5
37	5.0
45	5.0

Data-dependent mass measurements were performed with a Synapt G2-S HDMS (Waters), with an ESI source and a TOF detector, in positive resolution mode. Masses in a range of 50 to 3000 *m/z* were detected with 0.5 s per scan and leucine enkephalin being injected as a reference mass every 30 s. Used parameters: lockspray capillary current 2.5 kV, capillary current 2.5 kV, cone voltage 30 V, source temperature 120 °C, cone gas flow 60 l/h, flushing gas flow 550 l/h, with a temperature of 150 °C. Fragmentation in MS/MS mode was conducted via collision-induced dissociation (CID) with argon and a collision energy of 10-25 V. Fragmentation was started when the intensity of a mass exceeded 6000 counts/s and was finished after 6 s at max. Fragmentation was stopped prematurely if the intensity fell below 6000 counts/s.

LC-coupled MS^E measurements. Experiments were performed in three biological replicates. Data-independent measurements were performed as described in the LC-MS/MS section with the modification that data was acquired in continuous MS^E mode and the collision energy was 14-45 V.

Molecular networking and spectra annotation. Fragmentation spectra were converted from waters .raw to .mzXML using Proteowizard (ver. 3.0.9490), with 32-bit binary encoding precision and peak picking. Spectra were uploaded to the UCSD GNPS FTP-server [ucsd.gnps.edu] and investigated via the METBOLOMICS-SNETS (19) workflow with following parameters: parent mass tolerance 2 Da, ion tolerance 0.5 Da, minimal pairs cos 0.7, network topK 10, maximum connected component size 100, minimum matched peaks 6, minimum cluster size 2, run MSCluster. Data were visualized via Cytoscape (ver. 3.3.0). Redundancies and adducts were cleared manually. Network nodes corresponding to the uninoculated media or solvent background, as well as nodes with less than three fragment spectra were excluded.
Metabolites were identified through comparison with standards, searching the GNPS database and through manual annotation of fragment spectra by generating candidate structures in ChemBioDraw Ultra (PerkinElmer, ver. 13.0.2.30.21). Files were uploaded to MetFrag and subjected to *in silico* fragmentation (20).

Colorimetric siderophore detection. A chromeazurol S (CAS) assay, as described by Schwyn and Neilands in 1986 was used (21). In brief, cell free culture supernatant was mixed in equal amounts with the reaction solution (15 µM $FeCl_3$, 150 µM CAS, 600 µM cetyl trimethylammonium bromide, 563 mM piperazin, pH 5.6). After 3 hours of equilibration the absorption at 660 nm was measured. Experiments were performed in five biological replicates.

Compound purification and characterization. All commercially available solvents and reagents were used without further purification. Deionized water was purified to 18.2 MΩ·cm on a Milli-Q Biocel water purification system (EMD Millipore). Deoxacalcimycin was obtained, along with known compounds calcimycin and cezomycin, from crude extract of *Streptomyces chartreusis* NRRL3882 cultivated in ISP2. The mycelial cake was removed by centrifugation and the supernatant of a 12 l culture was extracted with equal amounts of ethyl acetate. The organic extract was evaporated to dryness and the remaining residue was dissolved in CH_3OH to give 10 mg/ml. Automated reversed-phase medium pressure liquid chromatography (RP-MPLC) was performed on a Combi*Flash* Rf (Teledyne Isco) using a 40 g SiliaSep™

C_{18} column (40-63 µm, 60 Å, Silicycle). The following H_2O/acetonitrile gradient with 0.1% FA with a flow rate of 40 ml/min was used for flash chromatography, while calcimycin-like compounds were detected at 360 nm.

Gradient for flash chromatography

Time [min]	% ACN with 0.1% FA
Initial	4.8
3	4.8
25	99.5
40	99.5

Peak fractions were combined, dried and subjected to further analysis. Ultra-performance liquid chromatography–high-resolution mass spectrometry (UPLC-HRMS) was performed using an Exactive Orbitrap mass spectrometer (Thermo Fisher Scientific) equipped with an Accella PDA (Thermo Fisher Scientific) and a SEDEX Model 80 LT-ELSD detector (Sedere). The UPLC was equipped with a Core Shell Kinetex C_{18} column (2.1 × 50 mm, 1.7 µm, Phenomenex). The gradient program involved a linear gradient at a flow rate of 500 µl/min from 95 % H_2O (0,1% FA) at 0.2 min to 100 % CH_3CN (0.1% FA) at 4.8 min, which was held for 3.2 min. The final amount of pure deoxacalcimycin was 2.94 mg.
All ^1H and ^{13}C NMR spectra were acquired on a 600 MHz Bruker Avance III NMR spectrometer (Billerica) operating at 600 and 150 MHz, respectively. All chemical shifts are reported in δ units and are referenced to the residual solvent signal of $CDCl_3$ (δ_H 7.26 ppm and δ_C 77.16 ppm). Coupling constants are reported in Hz with the following abbreviations: (s) singlet, (d) doublet, (t) triplet, (q) quartet, (m) multiplet, (br) broad, (app.) apparent. Optical rotations were recorded on an Autopol III polarimeter (Rudolph Research Analytical). Infrared spectra were acquired by attenuated total reflectance using a SMART iTR™ accessory on a Nicolet™ 6700 FTIR spectrometer (Thermo Fisher Scientific).

References

1. Wu Q, Liang J, Lin S, Zhou X, Bai L, Deng Z, Wang Z (2010) Characterization of the biosynthesis gene cluster for the pyrrole polyether antibiotic calcimycin (A23187) in *Streptomycs chartreusis* NRRL 3882. *Antimicrob Agents Chemother* 55(3):974-982.
2. Wu Q, Gou L, Lin S, Liang J, Yin J, Zhou X, Bai L, An D, Deng Z, Wang Z (2013) Characterization of the N-methyltransferase CalM involved in calcimycin biosynthesis by *Streptomyces chartreusis* NRRL 3882. *Biochimie* 95(7):1487-1493.
3. Barona-Gomez F, Wong U, Giannakopulos AE, Derrick PJ, Challis GL (2004) Identification of a cluster of genes that directs desferrioxamine biosynthesis in *Streptomyces coelicolor* M145. *J Am Chem Soc* 126(50):16282-16283.
4. Feistner GJ, Stahl DC, Gabrik AH (1993) Proferrioxamine siderophores of *Erwinia amylovora*. A capillary liquid chromatographic/electrospray tandem mass spectrometric study. *J Mass Spectrom* 28(3):163-175.
5. Adapa S, Hubts P, Keller-Schierlein W (1982) Metabolites of microorganisms. 216 Isolation structure and synthesis of ferrioxamine H. *Helvetica Chimica Acta* 65(6):1818-1824.
6. Takahashi A, Nakamura H, Kameyama T, Kurasawa S, Naganawa H, Okami Y, Takeuchi T, Umezawa H, Iitaka Y (1987) Bisucaberin, a new siderophore, sensitizing tumor cells to macrophage-mediated cytolysis. II. Physico-chemical properties and structure determination. *J Antibiot (Tokyo)* 40(12):1671-1676.
7. Telfer TJ, Gotsbacher MP, Soe CZ, Codd R (2016) Mixing up the pieces of the desferrioxamine B jigsaw defines the biosynthetic sequence catalyzed by DesD. *ACS Chem Biol* 11(5):1452-1462.
8. Challis GL, Ravel J (2000) Coelichelin, a new peptide siderophore encoded by the *Streptomyces coelicolor* genome: structure prediction from the sequence of its non-ribosomal peptide synthetase. *FEMS Microbiol Lett* 187(2):111-114.
9. Deitz WH, Bailey JH, Froelich EJ (1963) *In vitro* antibacterial properties of nalidixic acid, a new drug active against gram-negative organisms. *Antimicrob Agents Chemother* (Bethesda) 161:583-587.
10. Kieser T, Bibb MJ, Buttner MJ, Chater KF, Hopwood DA (2000) Practical *Streptomyces* genetics. (John Innes Foundation, Norwich) 412.
11. Stülke J, Hanschke R, Hecker M (1993) Temporal activation of beta-glucanase synthesis in *Bacillus subtilis* is mediated by the GTP pool. *J Gen Microbiol* 139(9):2041-2045.
12. Shirling EB, Gottlieb D (1966) Methods for characterization of Streptomyces species. *Int J Syst Bacteriol* 16:313-340.
13. Schwientek P, Szczepanowski R, Rückert C, Stoye J, Pühler A (2011) Sequencing of high G+C microbial genomes using the ultrafast pyrosequencing technology. *J Biotechnol* 155(1):68-77.
14. Wibberg D, Al-Dilaimi A, Busche T, Wedderhoff I, Schrempf H, Kalinowski J, Ortiz de Orué Lucana D (2016) Complete genome sequence of *Streptomyces reticuli*, an efficient degrader of crystalline cellulose. *J Biotechnol* 222:11-12.
15. Seemann T (2014) Prokka: Rapid prokaryotic genome annotation. *Bioinformatics* 30(14):2068-2069.
16. Meyer F, Goesmann A, McHardy AC, Bartels D, Bekel T, Clausen J, Kalinowski J, Linke B, Rupp O, Giegerich R, Pühler A (2003) GenDB-an open source genome annotation system for prokaryote genomes. *Nucleic Acids Res* 31(8):2187-2195.
17. Weber T, Blin K, Duddela S, Krug D, Kim HU, Bruccoleri R, Lee SY, Fischbach MA, Müller R, Wohlleben W, Breitling R, Takano E, Medema MH (2015) antiSMASH 3.0-a comprehensive resource for the genome mining of biosynthetic gene clusters. *Nucleic Acids Res* 43(W1):W237-W243.
18. Han AW, Sany M, Fishman B, Trindade-Silva AE, Soares CA, Distel DL, Butler A, Haygood MG (2013) Turnerbactin, a novel tricatecholate siderophore from the shipworm endosymbiont *Teredinibacter turnerae* T7901. *Plos One* 8(19):e76151.
19. Wang M, Carver JJ, Phelan VV, Sanchez LM, Garg N, Peng Y, Nguyen DD, Watrous J, Kapono CA, Luzzatto-Knaan T, Porto C, Bouslimani A, Melnik AV, Meehan MJ, Liu WT, Crüsemann M, Boudreau PD, Esquenazi E, Sandoval-Calderón M, Kersten RD, Pace LA, Quinn RA, Duncan KR, Hsu CC, Floros DJ, Gavilan RG, Kleigrewe K, Northen T, Dutton RJ, Parrot D, Carlson EE, Aigle B, Michelsen CF, Jelsbak L, Sohlenkamp C, Pevzner P, Edlund A, McLean J, Piel J, Murphy BT, Gerwick L, Liaw CC, Yang YL, Humpf HU, Maansson M, Keyzers RA, Sims AC, Johnson AR, Sidebottom AM, Sedio BE, Klitgaard A, Larson CB, Boya P CA, Torres-Mendoza D, Gonzalez DJ, Silva DB, Marques LM, Demarque DP, Pociute E, O'Neill EC, Briand E, Helfrich EJ, Granatosky EA, Glukhov E, Ryffel F, Houson H, Mohimani H, Kharbush JJ, Zeng Y, Vorholt JA, Kurita KL, Charusanti P, McPhail KL, Nielsen KF, Vuong L, Elfeki M, Traxler MF, Engene N, Koyama N, Vining OB, Baric R, Silva RR, Mascuch SJ, Tomasi S, Jenkins S, Macherla V, Hoffman T, Agarwal V, Williams PG, Dai J, Neupane R, Gurr J, Rodríguez AM, Lamsa A, Zhang C, Dorrestein K, Duggan BM, Almaliti J, Allard PM, Phapale P, Nothias LF, Alexandrov T, Litaudon M, Wolfender JL, Kyle JE, Metz TO, Peryea T, Nguyen DT, VanLeer D, Shinn P, Jadhav A, Müller R, Waters KM, Shi W, Liu X, Zhang L, Knight R, Jensen PR, Palsson BØ, Pogliano K, Linington RG, Gutiérrez M, Lopes NP, Gerwick WH, Moore BS, Dorrestein PC, Bandeira N (2016) Sharing and community curation of mass spectrometry data with Global Natural Products Social Molecular Networking. *Nat Biotechnol* 34(8):828-837.
20. Ruttkies C, Gehrlich M, Neumann S (2013) Tackling CASMI 2012: Solutions from MetFrag and MetFusion. *Metabolites* 3(3):623-636.
21. Schwyn B, Neilands JB (1987) Universal chemical assay for the detection and determination of siderophores. *Anal Biochem* 160(1):47-56.